The impact of Wind Farms on Subsynchronous Resonance in Power Systems

Elforsk rapport 11:29

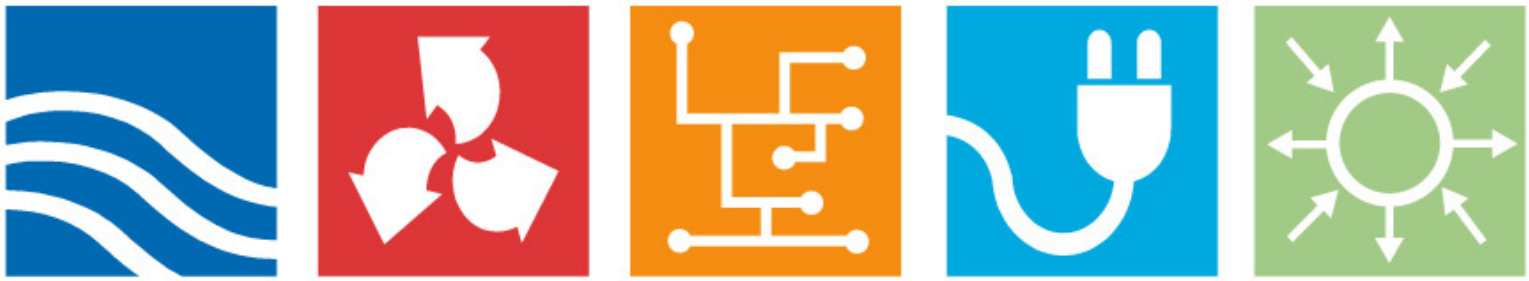

Masssimo Bongiorno, Andreas Petersson and Evert Agneholm April 2011

Vindforsk Energimyndigheten ELFORSK

The impact of Wind Farms on Subsynchronous Resonance in Power Systems

Elforsk rapport 11:29

Massimo Bongiorno, Andreas Petersson and Evert Agneholm April 2011

Preface

The purpose of this project is to investigate the potential risk for subsynchronous resonance (SSR) in case of large wind farms connected to series-compensated transmission lines. In particular, the focus of this project is on the risk for SSR in case of wind farms constituted by variable-speed wind turbines (mainly Doubly-Fed Induction Generator, DFIG).

The work was carried out by Massimo Bongiorno, Andreas Petersson and Evert Agneholm at Gothia Power as a project within the Swedish wind energy research programme "Vindforsk – II". The report is the final report for project V-309.

Vindforsk – III is funded by ABB, Arise windpower, AQSystem, E.ON Elnät, E.ON Vind Sverige, EBL-kompetanse, Falkenberg Energi, Fortum, Fred. Olsen Renwables, Gothia wind, Göteborg Energi, HS Kraft, Jämtkraft, Karlstads Energi, Luleå Energi, Mälarenergi, o2 Vindkompaniet, Rabbalshede Kraft, Skellefteå Kraft, Statkraft, Stena Renewable, Svenska Kraftnät, Tekniska Verken i Linköping, Triventus, Wallenstam, Varberg Energi, Vattenfall Vindkraft, Vestas Northern Europe, Öresundskraft and the Swedish Energy Agency.

Comments on the work and the final report have been given by a reference group with the following members: Philip Kjær from Vestas, Urban Axelsson from Vattenfall, Åke Petersson (substituted by Carl Heyman in the final part of the project) from ABB and Niclas Schönborg from Svenska Kraftnät (SvK).

Stockholm May 2011

Anders Björck

Programme maganger Vindforsk-III

Electricity- and heatproduction, Elforsk

Summary

Wind energy is one of the fastest growing renewable sources and thousands of MW are planned to be installed in Sweden. For this reason, the impact of wind power units, particularly when clustered as large wind farms, on the dynamics of the power systems must be carefully investigated. The aim of this project is to perform a preliminary study on the impact of wind farms on the risk of subsynchronous resonances in the power system when connected to series-compensated transmission lines. In particular, the focus of the project is on variable-speed wind turbines (full-power converter and doubly-fed induction generator, DFIG). As will be briefly discussed, variable-speed full-power-converter turbines seems to be immune to the phenomena, thanks to the decoupling between the generator and the transmission line offered by the back-to-back converter. The latter consideration also holds for wind farms connected to the power systems through HVDC systems, given a proper control of the HVDC system. Different considerations hold for the DFIG type. Through frequency scanning analysis, it will be shown that this type of wind turbines present a resonant condition at frequencies below the synchronous one. If a matching frequency exists in the transmission network due to the presence of the series capacitors, the system might become unstable and growing subsynchronous oscillations will be experienced. The resonant frequency of the DFIG is highly dependent on the converters (both the rotor-side and the grid-side converter) controller parameters as well as on the operating conditions. This dependency leads to a fairly wide range of frequencies, meaning that resonance can occur for a wide range of series compensation level.

Sammanfattning

Vindkraft är en av de snabbast växande förnybara energikällorna och det finns planer på att ansluta tusentals MW till det Svenska kraftsystemet. På grund av denna storskaliga integration är det viktigt att noga studera hur detta kommer att påverka dynamiken i kraftsystemet, speciellt då vindkraftverken kopplas samman i större vindkraftparker. Målsättningen med detta projekt är att göra en förstudie över om vindkraftverk kan orsaka subsynkron resonans när de är kopplade till en seriekompenserad transmissionsledning. Detta projekt fokuserar på vindkraftverk med variabelt varvtal (fulleffektomformare, dubbelmatade asynkrongeneratorer, så kallade DFIG). Som beskrivs i rapporten verkar vindkraftverk med variabelt varvtal och fulleffektomformare vara immuna mot subsynkron resonans eftersom generatorn och transmissionsledningarna blir särkopplade av omformarna. Detta gäller även för vindkraftsparker kopplade till kraftsystemet med hjälp av en HVDC länk, under förutsättningen att HVDC länken har ett lämpligt reglersystem. För DFIG systemen blir det dock annorlunda. Genom ”frekvensskanningsanalys”, visas det att denna typ av turbiner har en resonansfrekvens som ligger under den synkrona frekvensen 50 Hz. Om en matchande frekvens finns i transmissionssystemet, på grund av en seriekompensering, kan systemet bli instabilt med en växande subsynkron oscillation. DFIG systemets resonansfrekvens beror på omformarnas (både rotor- och nätomformaren) reglerparametrar och dess driftområde. Detta beroende leder till ett ganska stort område som resonansfrekvensen kan variera inom vilket innebär att resonans kan inträffa för flera olika seriekompenseringsnivåer.

Contents

1 Introduction

1.1 Background and aim of this project

Over the past few years, wind energy has shown the fastest growth amongst different sources of electric power generation [1,2]. This has led to several challenges in the large-scale integration of the wind farms in the existing transmission and distribution networks [3,4]. One of these is the need for substantial upgrade of grid transmission infrastructure including construction of new transmission lines (both AC and DC) to accommodate the increased power flow from the wind plants [5]. It is well known that series compensation is an effective means of enhancing the power transfer capability of existing transmission lines. Hence, series compensation is being increasingly considered for integrating large wind generation plants [6-8]. However, capacitors in series with transmission lines may cause subsynchronous resonance (SSR) which can lead to electrical instability at subsynchronous frequencies and potential turbine-generator shaft failure [9-11]. SSR is a condition where the electric network exchanges significant energy with a turbine-generator at one or more frequencies below the synchronous frequency f_0, defined as the frequency corresponding to the rotor average speed. There are two aspects of the SSR:

i) Self excitation involving both induction generator effect (IGE) and torsional interaction (TI),

ii) Transient torque (also called torque amplification, TA).

Although globally recognized as a dangerous condition for synchronous generators (mainly, steam and nuclear generation units), at the time when this project was proposed not so much research was conducted in case of wind farms connected to series compensated transmission lines. However, recent events have shown that if wind turbine generators are radially connected to series compensated transmission lines, there is a potential for SSR conditions, mainly due to self-excitation of the induction generators with increased level of series compensation [12,13]. The mechanical drive train of wind turbine generator system may also be susceptible to torsional vibrations which can be excited by both mechanical and electrical disturbances [14].

The aim of this project is to investigate the potential risk for subsynchronous resonance in case of large wind farms connected to series-compensated transmission lines. In particular, the focus of this project will be on wind farms constituted by variable-speed wind turbines (mainly Doubly-Fed Induction Generator, DFIG). Conditions that might lead to potential risk for SSR condition will be discussed and investigated. The impact of the different parts that constitute the control system for the DFIG system on possible resonant conditions with the network will be treated.

1.2 Outline of the report

After this introductory chapter, this report is organized as following:

- Chapter 2 presents an overview of the problem of SSR in power systems. Definition and classification of different types of SSR as well as methods for SSR investigation are discussed. Finally, the different countermeasures that generally can be taken to avoid the risk for SSR are described.
- Chapter 3 gives an overview of the problem of subsynchronous resonance in wind farms. The risk for subsynchronous resonance in case of wind farms constituted by the three main type of turbines (fixed speed, full-power converter and doubly-fed induction generator, DFIG, type), is briefly described. Being the main focus of this report, particular emphasis is addressed to the DFIG system.
- Chapter 4 presents the adopted model for the DFIG wind turbine. The different parts that constitute the control system of this turbine will be described in detail.
- Chapter 5 describes the adopted method for the evaluation of SSR in wind farms constituted by DFIG wind turbines. Obtained results are here presented.
- Chapter 6 presents the overall conclusions for this work and give some suggestions for future works.

2 Subsynchronous resonance in power systems

This chapter presents an overview of the problem of SSR in power systems. Definition and classification of different types of SSR will be given. Different countermeasures to the SSR problem will be described. Although considered a problem related to synchronous generators only, this overview is useful to understand the risk for SSR also in wind farms.

2.1 Introduction

Series compensation of long transmission lines is a cost-effective solution to enhance the power transfer and improve system stability. It was generally believed until 1971 that series compensation up to 70% of the total inductive reactance of the transmission line could be applied with little concern [15]. Usually, only problems related to protection and thermal issues were taken into account. However, it was in 1971 that system designers learned that the use of series compensation can lead to adverse phenomena on turbine-generator units connected to a series-compensated transmission line. These phenomena are related to a resonant condition leading to an energy exchange between the generation unit and the transmission line. As a result, oscillations having a characteristic frequency below the fundamental frequency of the power system (synchronous frequency) can be experienced. Therefore, this resonance condition has been named subsynchronous resonance (SSR) [16].

The SSR phenomenon was first recognized in the Mohave Project in 1970 [17]. The Mohave Project consisted of a 750 MVA cross-compound generation unit located in southern Nevada. Fig. 1 shows the single-line diagram of the power system in the Mohave area at that time. In 1970, shaft damage was experienced when opening the circuit breaker indicated in the figure; thus, when the Mohave generation unit became radially connected to the southern California Lugo bus. At that time, the power system operators did not recognize the problem and the generation unit was placed back in operation after a few months. Thus, a nearly identical incident occurred one year later, in 1971. For each event, the unit was shut down manually by the site operators. The operators observed flickering lights in the control room, vibration of the control room floor, excessive field current and alarm of excessive vibrations in the generator-shaft system, which continued for a few minutes. It was found that the shaft section in the slip rings area of the high-pressure turbine experienced extreme heating due to cycling torsional stress. Due to the excessive heat, the insulation in the slip rings area of the generator failed, resulting in an electric arc to ground of the generator field lead. Furthermore, a metallurgical analysis showed that the shaft material had experienced high stress, leading to plasticity of the material.

After a subsequent analysis of the phenomenon, it was found that the event experienced in the Mohave Project was due to an energy exchange between

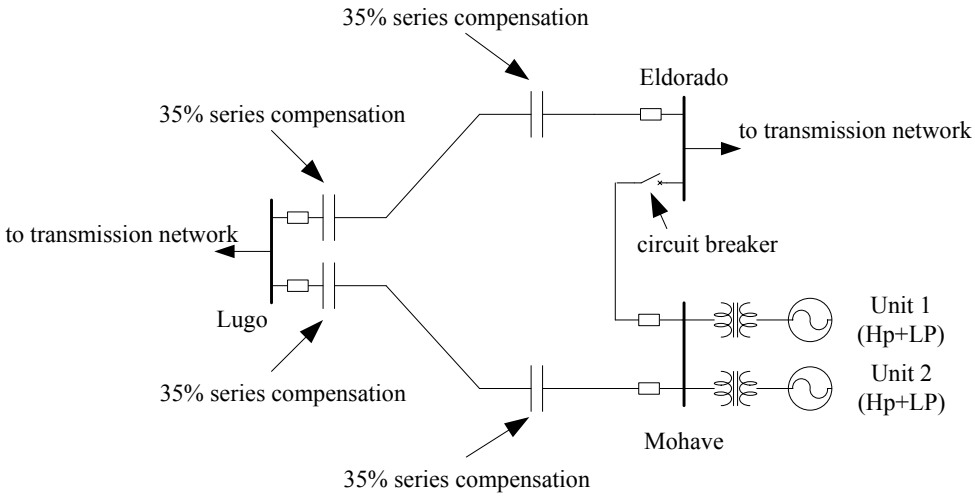

Fig. 1. Single-line diagram of the power system in the Mohave area in 1970.

the series-compensated line and the mechanical system of the Mohave power plant. These oscillations, due to the new power system condition when the circuit breaker was open, built up from a steady-state condition and led to growing shaft torque oscillations at one of the natural frequencies of the generator shaft.

After the two incidents in the Mohave Project, great effort has been directed from the research community and power system utilities to avoid the risk of SSR during system operation. Furthermore, the IEEE instituted a working group to define and classify the different types of SSR that can occur in a power system.

2.2 SSR definition and classification

According with the IEEE definition [16], SSR is defined as:

an electric power system condition where the electric network exchanges energy with a turbine generator at one or more of the natural frequencies of the combined system below the synchronous frequency of the system.

SSR is typically classified into two main groups: steady-state SSR (induction generator effect, IGE, and torsional interaction effect, TI) and transient torques (also known under the name of torque amplification, TA). In particular:

- **Induction generator effect (IGE).** IGE is a pure electrical phenomenon taking place at frequencies very close to the rated network frequency and in power systems having high degree of series compensation. In particular, IGE is caused by self excitation of the electrical system and does not involve the mechanical system of the generation unit. The resistance of the rotor to subsynchronous currents, viewed from the armature terminals, is negative [15]. For the same currents, the network presents a positive resistance. If the

negative resistance of the generator is greater in magnitude than the resistance of the network, sustained subsynchronous currents will be induced. In principle, IGE may occur in all kind of power generating plants, even for hydro-generator units. Although of academic interest, this form of SSR is rarely encountered in actual synchronous generators connected to the power systems and for this reason is not typically treated in scientific publications. However, it is of importance to stress that SSR due to IGE can be encountered in induction generators. Furthermore, as it will be mentioned further in this report, this kind of SSR can be experienced in wind turbines.

- **Torsional interaction effect (TI).** TI is an unstable condition that denotes an energy exchange between the electric power system and the generator shaft. In particular, TI occurs when the induced subsynchronous torque in the generator is electrically close to one of the natural frequencies of the generator shaft. When this happens, generator rotor oscillations will build up and this motion will induce armature voltage components at both subsynchronous (having frequency $f_0 - f_s$, where f_0 and f_s are the system frequency and the natural frequency of the generator shaft, respectively) and supersynchronous ($f_0 + f_s$) frequencies. If the resulting subsynchronous torque equals or exceeds the inherent mechanical damping of the rotor, the system will become self-excited. This kind of SSR does not occur in hydro-power stations, since the inertia of the hydro turbine is much smaller than the inertia of the generator (in the range of 5%). Therefore, when a torsional oscillation occurs in the shaft, the speed variation will almost totally be encountered on the hydro turbine, while the speed of the generator will remain approximately unaffected by the oscillation. As a result, the oscillation will not be recognized by the transmission system [18]. SSR due to TI effect can instead occur in thermal power plants, where the inertia of the turbine is in the same order of magnitude of the inertia of the generator. It is important to mention that SSR due to TI effect can also be experienced in case of large converters connected to a turbine generator. Typical examples are HVDC converter stations using both thyristor converters and transistor converters. In this case, when the converter station of the HVDC is operated as a rectifier, it will exhibit a negative resistance at certain subsynchronous frequencies, depending on the controller parameter settings [19]. If a matching resonant frequency exists in the power system, undamped oscillations might be experienced. For this reason, extensive SSR studies are typically performed when a new HVDC system is planned for installation in the vicinity of a series compensated transmission line.
- **Torque amplification (TA).** TA is the phenomenon that results from system disturbances. Each disturbance results in a sudden change in the current that will tend to oscillate. In case of non series-compensated lines, this will result in a dc offset that will decay with the subtransient and transient time constants of the generator. In a series-compensated line, instead, oscillations having a frequency corresponding to the resonance frequency of the network will be experienced. If the frequency of these oscillations coincides with one of

the natural frequencies of the generator shaft, large torques will be experienced. SSR due to TA can cause severe mechanical torsional oscillations in the shaft system connecting the generator and the turbines in thermal power plants.

Of the three types of interaction described above, the first two may be considered as small disturbance conditions (at least, initially). The third one, instead, is definitely not a small disturbance and in this case non-linearities of the power system must be taken into account in the analysis. From the system analysis point of view, it is important to observe that the induction generator effect and torsional interaction effects can be analyzed using linear models, while the mathematical analysis of the torque amplification effect is complex and cumbersome and is typically approached using simulation programs.

2.3 SSR investigation and analysis

As briefly pointed out in the previous section, several tools for SSR investigation and analysis are available and the applicability of one method in place of another one mainly depends on the nature of the SSR to be investigated. Among all possible methods, frequency scanning, eigenvalue analysis and electromagnetic transient analysis are the three most used methods both in the academia and in the industry. The electromagnetic transient analysis implies the utilization of simulation programs such as EMTP or PSCAD/EMTDC.

Frequency scanning and eigenvalue analysis are the preferred choice for investigation of SSR due to IGE and TI, since they are based on the utilization of linearized models both of the machine and of the power system. Frequency scanning can also indicate the risk for SSR due to torque amplification. Due to the complexity of the system equation when modeling, for example, short-circuit faults, electromagnetic transient analysis is instead preferred for investigate conditions that might lead to torque amplification.

2.4 Countermeasures to the SSR problem

As mentioned earlier in this chapter, all SSR phenomena cause stress on the shaft system in the turbine-generator string in the power plant. Without a fast action from the system operators, both mechanical and electrical damage can occur causing lack of available power and great economical losses. An extended analysis of possible countermeasures to avoid or mitigate the risk of SSR in the power system is carried out in [11]; the following is a brief summary.

2.4.1 Power system design improvements

SSR is a phenomenon that occurs under specific conditions in a series-compensated power system. A first solution to avoid the problem might be a proper choice of the series-compensation level to ensure that the network resonance frequency does not coincide with the complementary of one of the

natural frequencies of the generator shaft. Although effective, this solution is not feasible, since the value of the network impedance, thus its resonance frequency, varies depending on the operating conditions of the power system.

Alternatively, the use of shunt compensation can be employed instead of series compensation. It has been shown that shunt capacitors lead to resonances above the synchronous frequency (supersynchronous range) [11]. At these frequencies, the network presents a small positive damping, i.e. they do not represent a risk for the rotor shaft. However, the use of shunt compensation cannot completely replace the series compensation. The use of series compensation is more economically attractive and flexible. Furthermore, when series compensation is used, the angle deviation between the sending and the receiving ends of the transmission lines decreases. This improves the synchronizing strength of the power system.

When possible, it is convenient to always use a combination of shunt and series compensation.

2.4.2 Turbine-generator design improvements

The possibilities for improvements in this area are limited. Of course, it is straightforward to imagine to design the machines so that the lowest torsional frequency of the shaft system is greater than the synchronous frequency (i.e., natural frequencies of the generator-shaft system only in the supersynchronous range). This is impractical due to constraints on shaft and bearing size. The natural frequencies of the shaft can typically be varied only within a small limit. However, this will not have a greater impact on the SSR problem, due to the uncertainty of the resonant frequency of the network. Use of pole-face damping windings can reduce the negative resistance of the generator seen from the machine terminals [11]. This solution is relatively inexpensive and can be easily installed in new machines. However, it is impractical to install such windings in old machines. Moreover, this solution is effective only against SSR due to IGE, while it does not have any impact on mitigation of SSR due to TI and TA.

2.4.3 Use of auxiliary devices

The most commonly applied method for SSR mitigation is to install an auxiliary (mitigation) device in the power system. It is mainly in this direction that the research community is moving towards. Here, a brief description of some possible solutions is given.

Blocking filter

A simple method to achieve SSR mitigation is to install a blocking filter in series with the generator step-up transformer winding [21]. Typically, the filter is connected on the neutral end of the high voltage side of the transformer, as shown in Fig. 2. Alternatively, the filter can be connected to the phases on the high voltage side of the step-up transformer. To protect the system against overvoltages, a protection device (such as a varistor, not shown for clarity of the figure) must be connected across the series filter.

This type of filter is meant to block the line current components having frequency $f_0 - f_m$. In practical installations, the rotor shaft has more than one natural frequency (i.e., the shaft is constituted by several turbine stages). In this case, the blocking filter will be constituted by several resonant circuits connected in series. Each filter will be tuned for one natural frequency of the generator-turbine shaft system. This solution is effective both for mitigation of SSR due to TI and TA and its performance is not affected by changes in the power system.

A disadvantage with this solution is that the tuning of the filter is dependent on the system frequency (which changes during normal operations and during fault conditions) and on the variation of the filter components value due to temperature and aging. Being implemented in the three-phase system, this lead to the need for wider filters (they cannot just be tuned for the specific resonant frequency); this might mean that this solution cannot be applied in case of SSR in wind farms, as it will be explained later in this report.

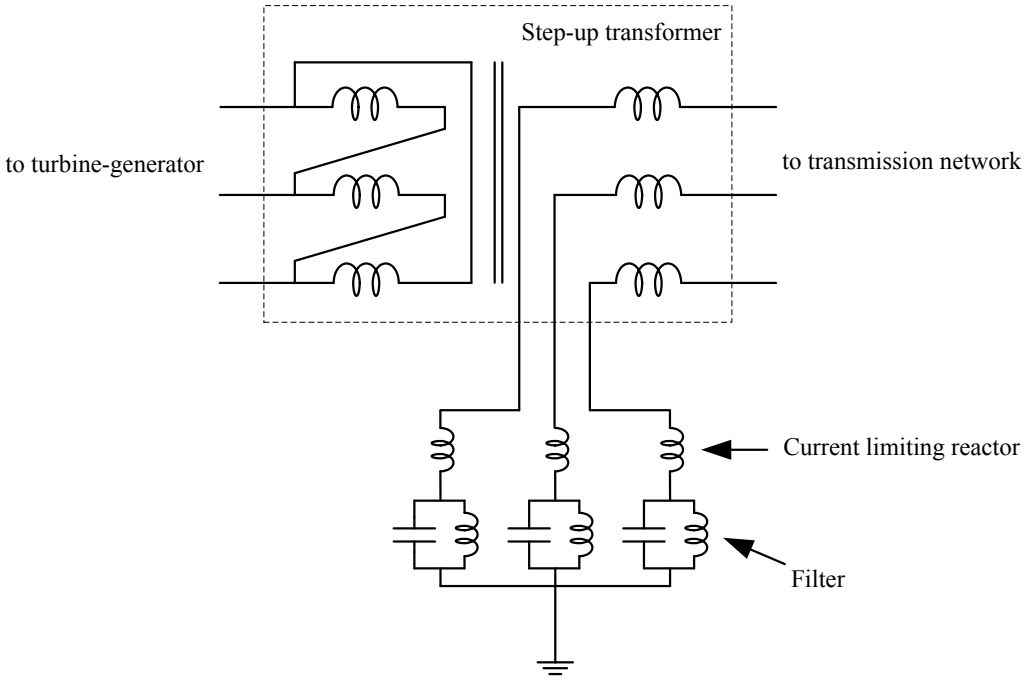

Fig. 2 - Three-line diagram of step-up transformer with blocking filter.

NGH-damping scheme

The NGH-damping scheme, depicted in Fig. 3, was first introduced by N. G. Hingorani in 1981 [22, 23] and consists of a resistor and a thyristor based ac switch connected in parallel with the series capacitor of the line.

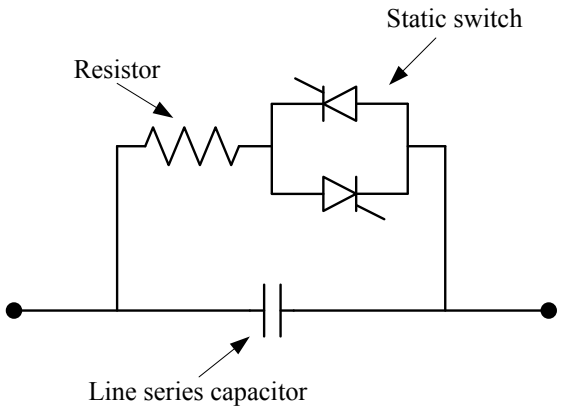

Fig. 3 - Single-line diagram of NGH-damping scheme.

To understand the principle of operations of the NGH-scheme for SSR mitigation, the curves depicted in Fig. 4 can be used. Consider a purely sinusoidal voltage waveform having characteristic frequency f_0 (either 50 or 60 Hz). In this case, two subsequent zero crossing will occur in a time equal to $1/(2f_0)$ (dashed curve). If the voltage is constituted by a fundamental and a subsynchronous component, some half cycles will be longer than $1/(2f_0)$, as it can be seen from the solid curve in the figure. The principle of the NGH-damping scheme is to dissipate capacitor charges over the resistor whenever the measured voltage half cycle period exceeds the rated value. This can be achieved by proper control of the static switch.

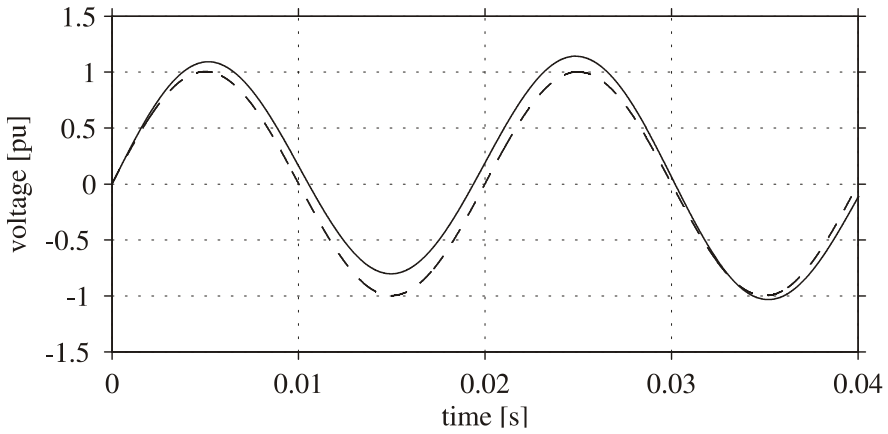

Fig. 4 - Comparison between fundamental voltage (dashed curve) and fundamental plus subsynchronous voltage (solid curve).

The control system operation is independent for each phase and does not require detection of a specific subsynchronous signal.

This solution is effective in mitigation of SSR both due to TI and TA. Furthermore, the NGH scheme can be used to protect the series capacitor against overvoltages. However, studies have shown that some undamping might occur for torsional modes that are not in resonance with the electrical system [11]. This must be taken into account when installing this type of

device. The NGH damping principle can be further extended to the basic TCSC (Thyristor Switched Series Capacitor) circuit structure, in order to make it immune to SSR.

FACTS devices

The actual trend for SSR mitigation is to install a FACTS device in the transmission line. There are several FACTS controllers that have been proposed and developed for this purpose. Typically, FACTS controllers are divided into two main categories: shunt-connected and series-connected devices. In particular, these categories include:

- **Shunt-connected FACTS devices:** this type of devices are controlled to inject (or absorb) reactive power to (from) the power systems by proper control of static semiconductor valves or switches. Among the shunt-connected FACTS devices, it is important to mention the Static Var Compensator (SVC), constituted by Thyristor Controlled Reactors (TCR), Thyristor Switched Capacitors (TSC) together with passive capacitive filter banks [23]. The SVC only is intended for reactive power control. A newer device for shunt compensation is the STATCOM [11, 24], which is based on VSC technology. The STATCOM can be equipped with energy storage for active power injection, which can be beneficial for damping operations.
- **Series-connected FACTS devices:** these types of devices are controlled to inject a voltage in series with the grid voltage. Among the series-connected FACTS devices, it is important to mention the Thyristor Controlled Switched Capacitor (TCSC) [25], the Thyristor Switched Series Capacitor (TSSC) [23] and the Static Synchronous Series Compensator (SSSC) [26,27].

Both in shunt and series connection, the effect of a FACTS device, seen from the generation unit terminals, is to dynamically modify the impedance of the power system. Therefore, FACTS devices represent an interesting solution to the problem of SSR mitigation. In particular, as compared with the shunt configuration, series-connected FACTS are generally considered more efficient in damping oscillations [23,11]. This holds for all kind of damping controllers and is mainly due to the direct relation between voltage and flux.

2.5 Conclusions

In this chapter, an overview of the problem of subsynchronous resonance (SSR) in power systems has been given. Methods available to investigate the potential risk for SSR in the power systems have been briefly discussed. Thus, different countermeasures to the SSR problem have been described. Nowadays, FACTS controllers are considered as one of the most attractive solutions for the problem of SSR in transmission networks. In the last decade, several researchers have put their attention to the development of novel control strategies for a cost-effective way of providing power system damping at frequencies below the fundamental. The overview carried out here is mainly related to synchronous generators connected to the grid. In the next chapter, the risk for SSR in wind farms will be treated.

3 Subsynchronous Resonance in Wind Farms

This chapter gives an overview of the problem of subsynchronous resonance in wind farms. The risk for subsynchronous resonance in case of wind farms constituted by the three main type of turbines (fixed speed, full-power converter and doubly-fed induction generator, DFIG, type), will be briefly described. Being the main focus of this report, particular emphasis will be addressed to the DFIG system.

3.1 Introduction

In the previous chapter, an overview of the problem of SSR was provided. Also, the tools that are typically used both in the research community as well as in the system utilities to investigate the potential risk for SSR have been briefly described. Finally, the actual countermeasures applicable to reduce the SSR risk have been listed. Being the focus of this work, this chapter deals with the risk for SSR in wind farms. As generally known, there are three main kinds of wind turbines: fixed speed, full-power converter and doubly-feed induction generator (DFIG). All these different types differ not only for the dynamical behavior at fundamental frequency, but also from a subsynchronous point of view. The following is a brief overview on the different kind of turbines and the associated potential risk for SSR. Special focus will be on the DFIG type, since this is the less investigated one and it is also the turbine topology that is installed in the Zorillo Gulf Wind Farm, where the first known incident for wind turbines related to SSR phenomena has occurred.

3.2 SSR in case of fixed-speed wind turbines

Fixed-speed wind turbines (WT) are typically constituted by an induction generator (IG) directly connected to the electrical grid, as depicted in Fig. 5. The rotor speed of the fixed-speed wind turbine is in principle determined by the grid frequency, the gearbox ratio and the pole-pair number of the generator. In order to limit the power to the turbine above rated wind speed, the blades of the fixed-speed WT are, typically, designed to stall at higher wind speeds, meaning that no pitch mechanism is necessary [28]. An advantage with stall control is that the power variation due to a wind gust is relatively small. On the other hand, the trust forces are relatively large. One way of fine adjusting the output power of the WT is to increase the pitch angle towards stall; this is referred to as active stall.

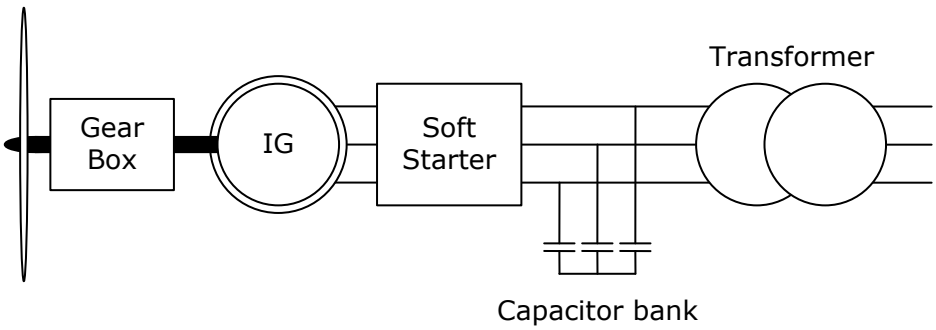

Fig. 5 - Fixed-speed wind turbine with an induction generator.

The fixed-speed WT system has often two fixed speeds. This is accomplished by using two generators with different ratings and pole pairs. Alternatively, a generator with two windings having different ratings and pole pairs can be used. This leads to increased aerodynamic capture as well as reduced magnetizing losses at low wind speeds [29]. Moreover, the system consists of a capacitor bank for compensating the reactive power consumption of the induction generator and a soft starter for smoothly connecting the generator to the grid. A variant of this turbine is the WT with variable slip, as depicted in Fig. 6. In this system, the IG has a wound rotor with external rotor resistances connected. This means that it is possible to temporarily vary the rotor speed. Therefore, in this kind of configuration, it is advantageous to use pitch control in order to limit the power above rated wind speed. This is due to the fact that the pitch control has relatively large power variations due to a wind gust, which can be stored as kinetic energy by changing the rotor speed. A major benefit of the pitch controlled system is that the trust forces acting on the turbine are relatively small, in contrast to the stall controlled system.

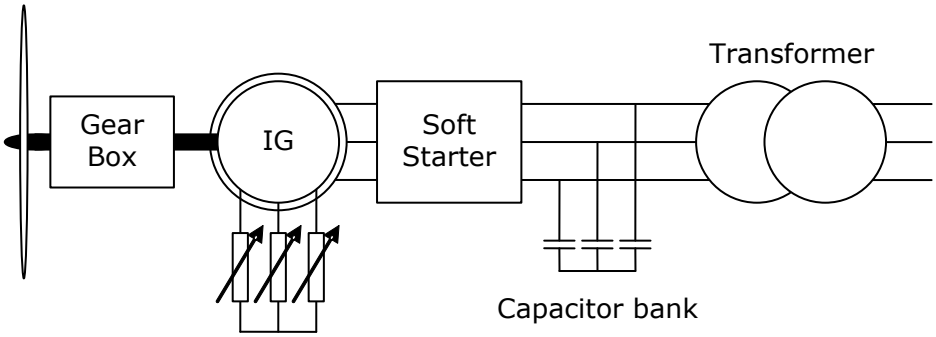

Fig. 6 - Fixed-speed wind turbine with an induction generator with variable slip.

It has been proven in [12,13,30] that SSR problems might arise in fixed speed wind turbines connected to series-compensated lines. This is mainly due to IGE in the machine electrical characteristics. In some specific conditions, SSR due to TI can also be triggered. Early wind turbines were of this type, but nowadays they are not so common. Therefore, investigation of

SSR for this kind of turbines has mainly an academic interest and will not be treated in this report.

3.3 SSR in case of full-power converter wind turbines

As mentioned in the previous section, fixed-speed wind turbines are not the preferred solution nowadays. Instead the actual trend goes in the direction of variable-speed wind turbines, i.e. wind turbine solutions that allow variable-speed operation. There are several reasons for using variable-speed operation of wind turbines; among those are possibilities to reduce stresses in the mechanical structure, acoustic noise reduction and the possibility to control active and reactive power [28]. This means that, in principle, all variable-speed WT are equipped with pitch control, which for instance reduces the trust forces on the WT. Power variations due to wind gust, as mentioned earlier, can easily be handled by varying the rotor speed. This means that power fluctuation caused by the wind is stored as kinetic energy in the rotor.

Fig. 7 shows a variable-speed WT with a full-power converter and a multiple-pole synchronous generator (SG). In this kind of solution, the wind turbine is connected to the mains through a back-to-back converter rated for the full power of the turbine system.

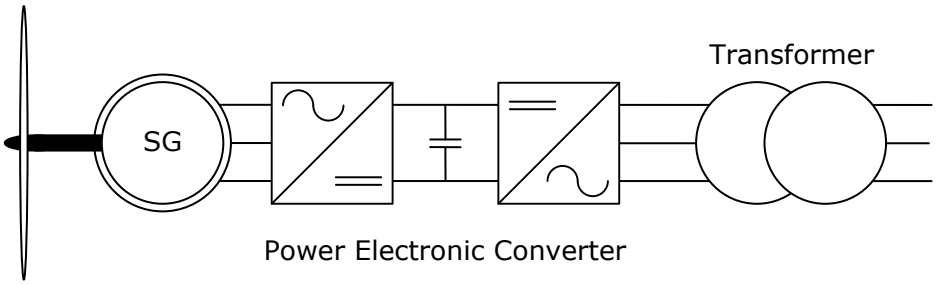

Fig. 7 - Variable-speed wind turbine with a full-power converter.

In this type of turbine, the presence of the back-to-back converter provides a decoupling between the grid and the turbine. Therefore, as long as the converter is operated within its linear range of operations and if an oscillation is triggered on the grid side of the converter it will not be reflected on the wind turbine side. For this reason, this type of turbine should not be affected by SSR problems. The same consideration holds for wind turbines connected to the power systems through HVDC links. HVDC links represent a risk for SSR mainly when operated as rectifiers [19]. Therefore, when power is delivered from the wind farm to the grid, the grid-side converter will operate as an inverter and thus will not contribute to the risk for SSR, since it will provide positive damping at subsynchronous frequencies. When operated in no-load conditions, the grid-side converter of the HVDC system will be operated as a rectifier to keep the dc-link voltage. In this case, carefulness must be taken in the controller design and the same design rules that apply for a HVDC link connected to a series-compensated line must be taken.

3.4 SSR in case of DFIG wind turbines

A variant of the variable-speed WT with a doubly-fed induction generator (DFIG) is shown in Fig. 8. In the DFIG system the stator is directly connected to the grid while the rotor winding is connected via slip rings to a back-to-back converter. For variable-speed systems with limited variable-speed range, e.g. ±30% of synchronous speed, the DFIG can be an interesting solution, since the power electronic converter only has to handle a fraction (30%) of the total power. This means that the losses in the power electronic converter can be reduced compared to a system where the converter has to handle the total power. In addition, the cost of the converter becomes lower.

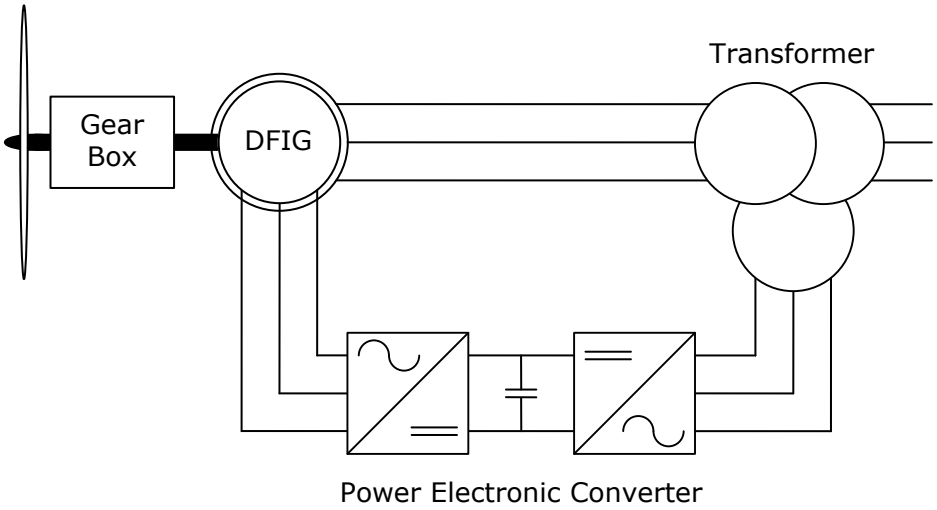

Fig. 8 - Variable-speed wind turbine with a doubly-fed induction generator (DFIG).

Until about two years ago, at the time of the writing the proposal for this project, it was a common believe that DFIG-based wind turbines were immune to the SSR phenomena, similar to the full power converter ones. This was mainly due to the ability of the control system for the DFIG system to control the torque and the speed of the turbine at frequencies below the fundamental. However, in October 2009 an incident in the Zorillo Gulf Wind farm (Texas), subsequently identified as an SSR event, has occurred. This is generally considered the first event of SSR between a DFIG-based wind farm and a series compensated transmission line. To understand what has happened in Texas in 2009, the partial single-line diagram of the power system around the wind farm is depicted in Fig. 9, while the simplified schematic of the 345kV system is depicted in Fig. 10 [32].

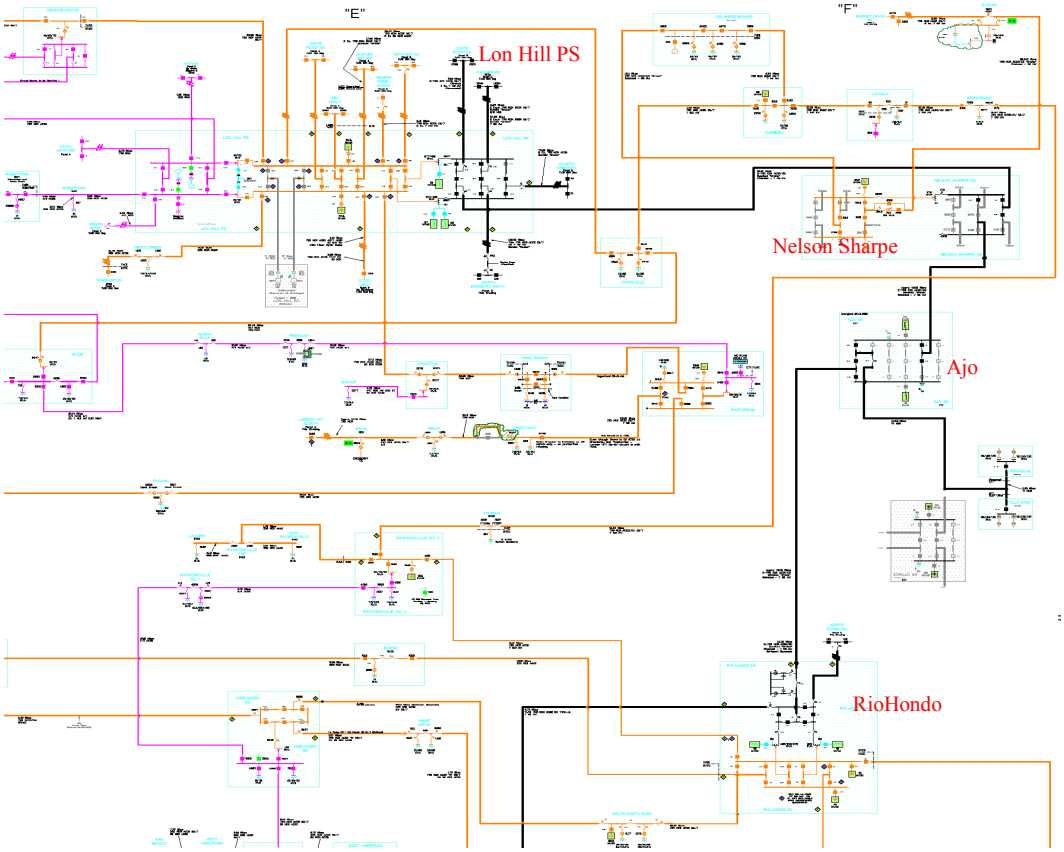

Fig. 9 - Simplified single-line diagram of the power system around the Zorillo Gulf Wind Farms in Texas.

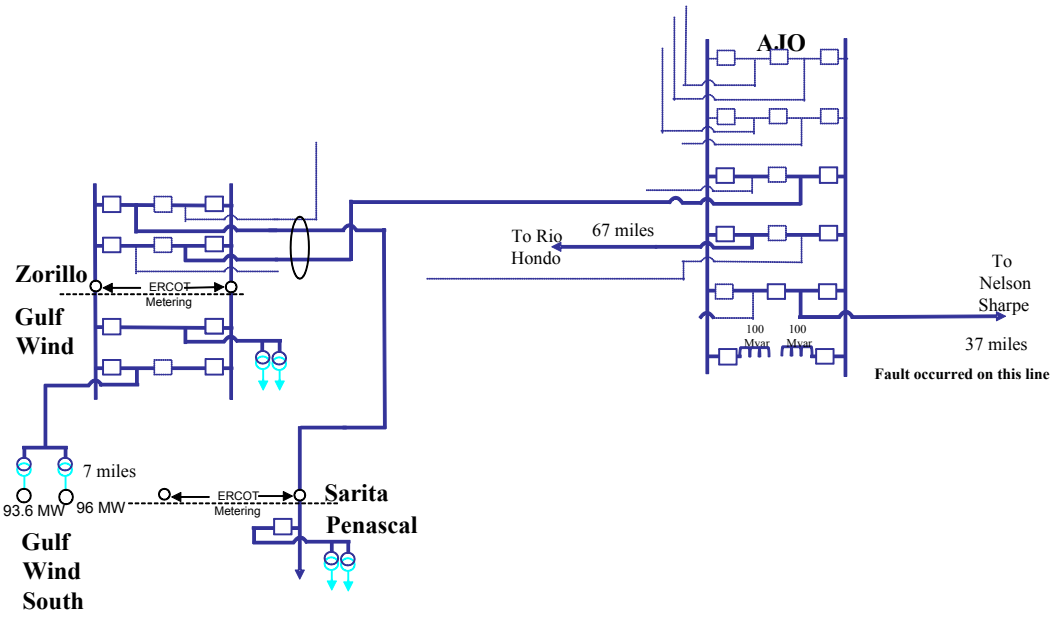

Fig. 10 - Detail of the 345kV system in the neighborhood of the Zorillo Gulf Wind Farms.

On the 10th of October 2009, a single-phase to ground fault in the 37 miles transmission line that goes from Ajo to Nelson Sharpe occurred. The initial fault was cleared in 2.5 cycles. Due to the operation of the circuit breakers in Ajo, the wind farms became radially connected to the Rio Hondo series compensated line. With this new network configuration, oscillations in the system voltage started to build up and shortly the system experienced a peak voltage up to about 195%. This resulted in the trip of the Rio Hondo to Ajo line and the shunt reactors at Ajo. Also, the series capacitors were bypassed approximately 1.5 seconds after the event. The series capacitor controls indicated subsynchronous currents during the event.

As a result of this event, crowbars were activitated in numerous turbines in both wind farms.

Figures 11 to 13 show the recordings of the event. It is clearly visible from the depicted waveforms that directly after the fault the system tends to instability and large oscillations have been experienced both in the voltage and in the current. From Fig. 12 and Fig. 13, the subsynchronous nature of the oscillations can be easily observed in the measured current (where the different dominating frequency in the measured waveforms between pre-fault and post-fault condition can be clearly appreciated) as well as in the measured voltage, where the amplitude of the signal is clearly modulated, denoting a subsynchronous component.

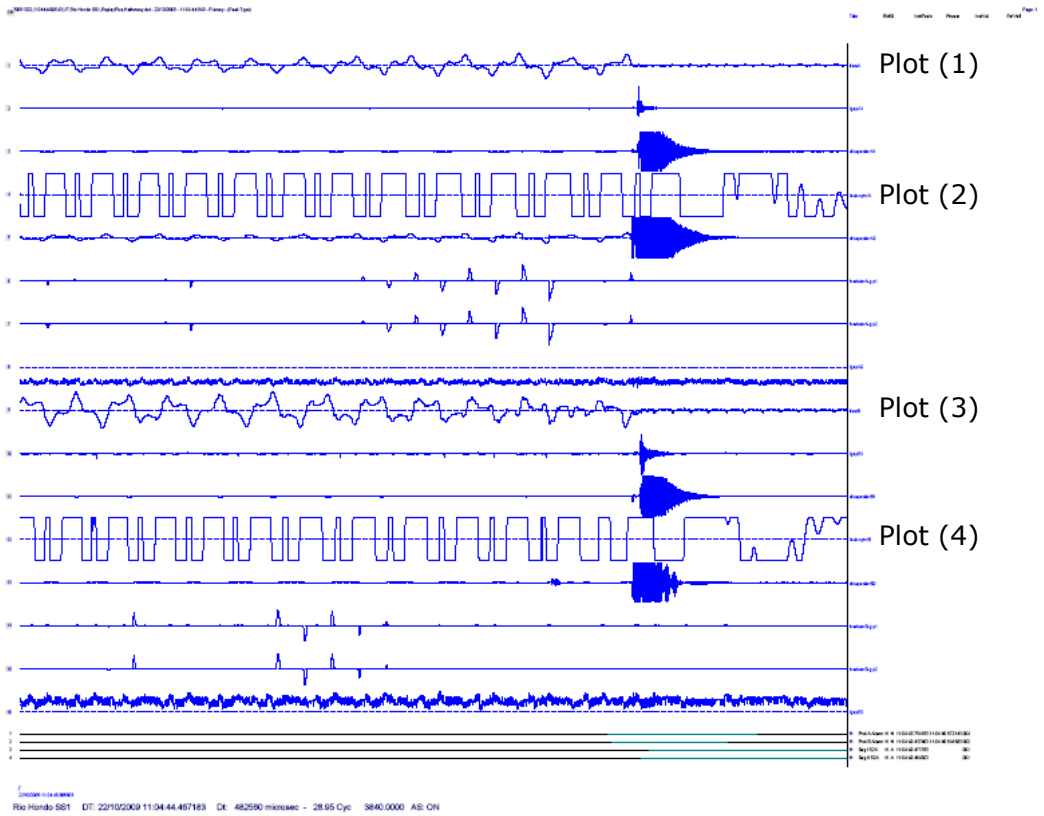

Fig. 11 - Measured quantities at the Rio Hondo series-capacitor banks. Plot (1): line current in phase *a*; Plot (2): subsynchronous current in phase *a*; Plot (3): line current in phase *b*; Plot (4)subsynchronous current in phase b. Additional measurements from the series-capacitor banks are also displayed in the figure.

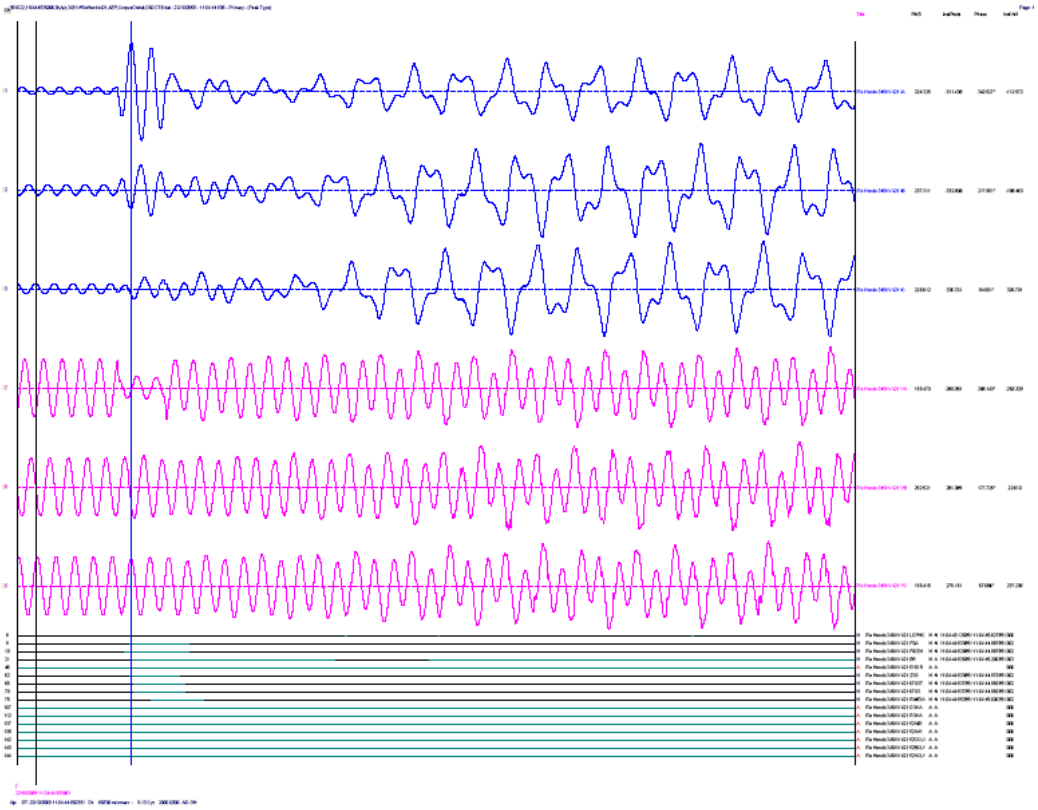

Fig. 12 - Measured quantities for the Rio Hondo SEL421 at Ajo. Waveforms from top to bottom: line current in phase *a*, line current in phase *b*, line current in phase *c*, phase voltage in phase *a*, phase voltage in phase *b*, phase voltage in phase *c*.

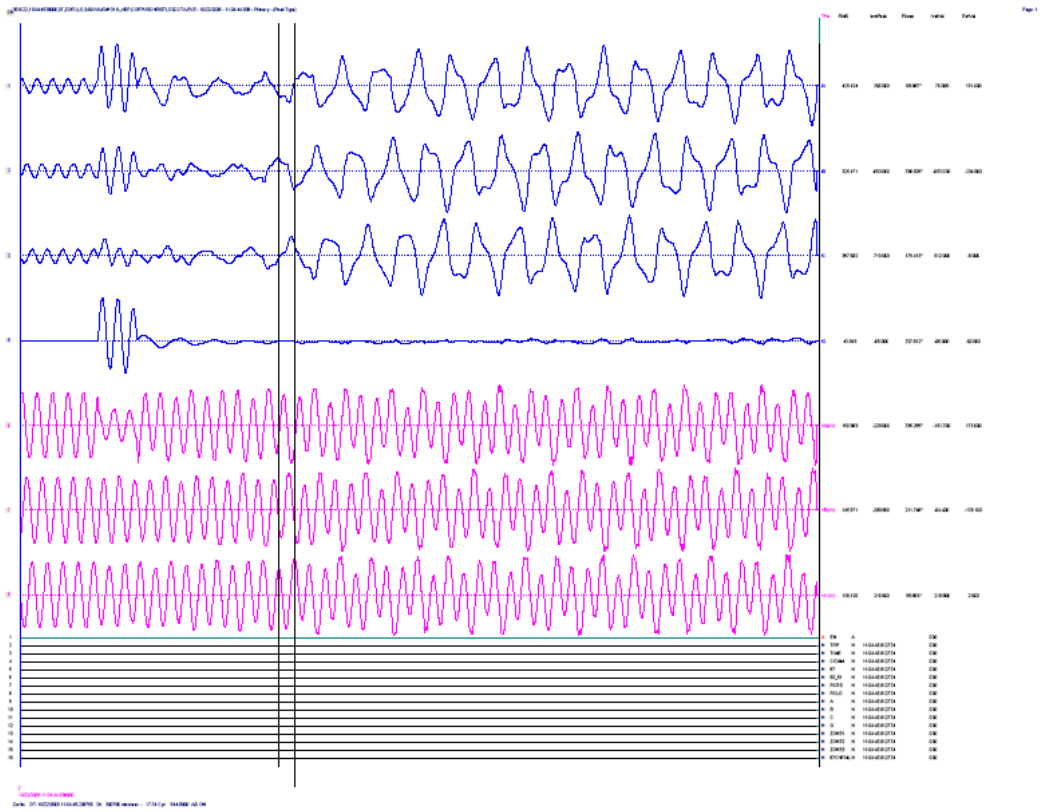

Fig. 13 - Measured quantities for the Ajo 311L at Zorillo. Waveforms from top to bottom: line current in phase *a*, line current in phase *b*, line current in phase *c*, phase voltage in phase *a*, phase voltage in phase *b*, phase voltage in phase *c*.

After this event, large effort has been addressed both from the research community and from the manufactures in order to understand the physical phenomena behind this phenomenon. Although it was evident that the incident was due to a SSR condition, but the principle that led to the event was not completely clear. In the following of this report, the authors will try to give a physical explanation of the event.

3.5 Conclusions

In this chapter, an overview of the risk for SSR conditions in case of wind farms connected to series-compensated transmission lines has been given. In particular, the risk for SSR in case of wind farms constituted by the three main topologies of turbines (fixed speed, full-power converter and doubly-fed induction generator, DFIG, type), has been briefly described. As discussed, fixed speed wind turbines might be affected by SSR when radially connected to a series compensated line, while (properly designed) variable-speed full-power converter turbines seems to be immune to the phenomenon. Particular focus shall be made for the DFIG type. This variable-speed turbine topology is the one employed in the Zorillo Gulf Wind Farm, the first wind farms where an event that could be identified as a SSR was observed. For this reason, and in

agreement with the members of the reference group for this project, the main focus of this report has been on this turbine topology. In order to properly investigate the phenomenon, it is of high importance to have a proper modeling of the DFIG and of the power system. In the following, the adopted model for the DFIG, including the main control algorithms, will be described.

4 Modeling and control of DFIG wind turbines

It has been shown in the previous chapter that SSR can be triggered in case of DFIG-based wind farms radially connected to series compensated transmission lines. To understand the nature of this phenomenon, it is of high importance to have a proper dynamic model of the DFIG system, including its control system. This chapter presents adopted DFIG model and the main parts that constitute the control system for the investigated wind turbine topology.

4.1 DFIG wind turbine

The control system of the DFIG wind turbine depends on pitch control and variable-speed operation of the generator. Above rated wind speed the pitch controller limits the incoming power to the rated. The generator is controlled to the rated power or torque. Below rated wind speed the pitch angle is set to maximize the captured power. The generator is in speed control and its reference value is set to maximize the aerodynamic efficiency.

4.2 Simulation model

In Fig 14 the PSCAD/EMTDC implementation of the wind turbine simulation model can be seen. As seen in the figure the model consists of a wound-rotor induction generator (i.e. the DFIG), a two-mass shaft model, a back-to-back power electronic converter with a dc-link, filters and a transformer.

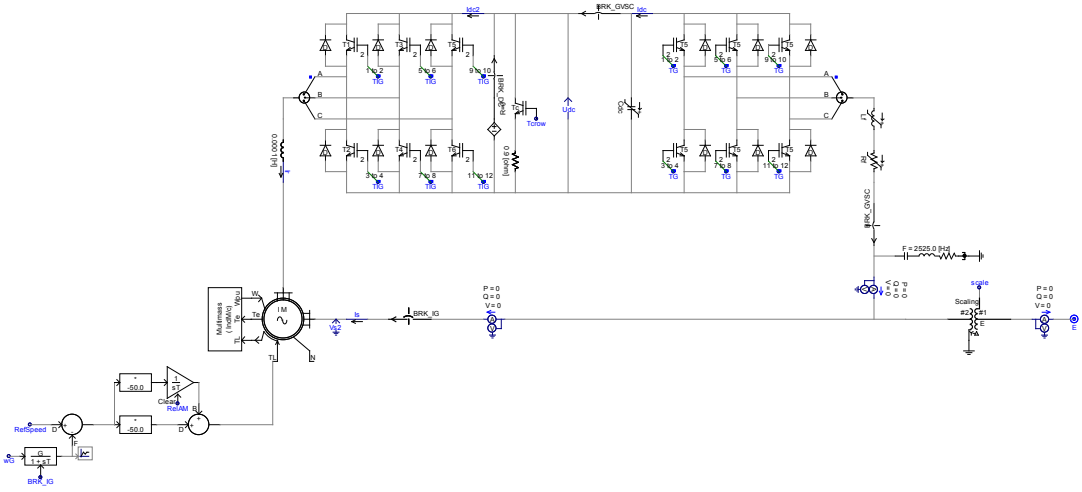

Fig. 14 – DFIG wind turbine model in PSCAD/EMTDC.

The converter is connected to the rotor circuit of the induction generator while the stator is directly connected to the step-up transformer and the grid. The transformer model that has been used can scale the turbine model to any

desirable power rating. The scaling transformer comes from the Elcatranix E-TRAN PSCAD library package.

The model of the turbine and the pitch controller has in this study been simplified. This means that here only a PI controller, controlling the rotor speed, models the turbine and supplies the torque to the drive train. The reason for this simplification is that that the wind speed and the pitch controller dynamics is slower (considered to be in the range of 1 Hz) than the SSR dynamics to be studied (40 to 50 Hz).

4.3 Control of the DFIG

In Fig. 15 an equivalent circuit of the DFIG system can be seen. The system consists of a DFIG and a back-to-back voltage source converter with a dc link. The back-to-back converter consists of a grid-side converter (GSC) and a machine-side converter (MSC). Moreover, a grid filter is placed in between the GSC and the grid, since both the grid and the voltage source converter are voltage stiff and to reduce the harmonics caused by the converter. For voltage source converters the grid filter used is mainly an *L*-filter or an *LCL*-filter. However, here the *L*-grid filter will be used, as shown in Fig. 15.

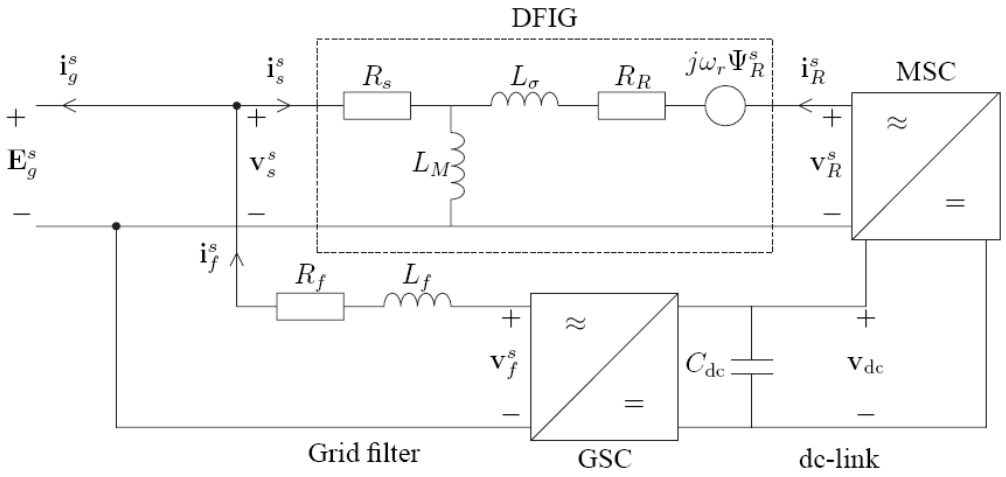

Fig. 15 – Equivalent circuit of the DFIG electrical circuit.

The MSC controls speed or torque of the DFIG while the main objective of the GSC is to keep the dc-link voltage constant. Both the MSC and the GSC has an internal fast current control loop. The currents are controlled by means of space vectors and are synchronized to the grid voltage by a phase-locked loop. Then, outer, slower control loops, are added to control the generator and the dc-link voltage. Figures Fig. 16 and Fig. 17 show the overall control schemes for the machine-side and for the grid-side converters, respectively. The meaning of each symbol in the two control schemes will be given when describing the individual controllers in the following sections. Below a description of the different controller used in this study are presented in more detail. The derivation of the control laws, in this chapter, can be somewhat succinctly explained. Though, the derivation is essentially following [29] where much more details can be found for the interested reader.

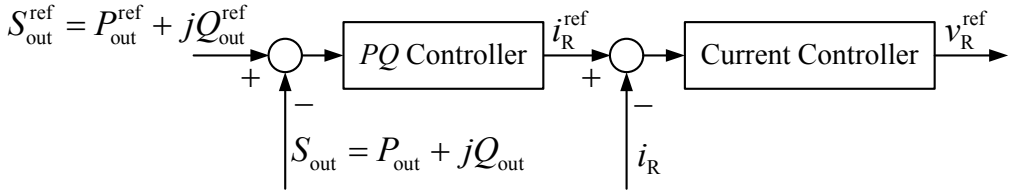

Fig. 16 – Machine-side converter control scheme.

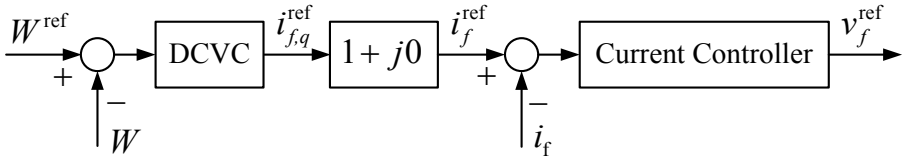

Fig. 17 – Grid-side converter control scheme.

4.3.1 Phase-Locked Loop (PLL)

The objective of the phase-locked loop (PLL) can be to estimate the angle and frequency of a signal, e.g., the synchronous frequency, ω_1, and its corresponding angle, θ_1. This is then used to synchronize the space vectors to the grid voltage. Here, the space vectors is synchronized in such a way that for a perfect field orientation the grid voltage is align with the *q*-axis. The PLL-type estimator used here is described by [37]:

$$\begin{aligned} \frac{d\hat{\omega}_1}{dt} &= \rho^2 \varepsilon \\ \frac{d\hat{\theta}_1}{dt} &= \hat{\omega}_1 + 2\rho\varepsilon \end{aligned} \tag{4.1}$$

where ρ is the bandwidth of the PLL, $\varepsilon = \sin(\theta_1 - \hat{\theta}_1)$ and $(\theta_1 - \hat{\theta}_1)$ is the error in the estimated angle. In this study ε is chosen as:

$$\begin{aligned} \varepsilon &= \frac{\text{Im}\left[j \cdot E_g e^{j(\theta_1 - \hat{\theta}_1)}\right]}{E_{nom}} \\ &= -\frac{\text{Re}\left[E_g e^{j(\theta_1 - \hat{\theta}_1)}\right]}{E_{nom}} \approx \left\{E_g \approx E_{nom}\right\} \approx \sin(\theta_1 - \hat{\theta}_1) \end{aligned} \tag{4.2}$$

In the equation above $E_g e^{j\theta_1}$ is the grid voltage and E_{nom} is the nominal grid voltage.

4.3.2 DC-link voltage control (DVCV)

The energy, W_{dc}, stored in the dc-link capacitor, C, can be expressed as

$$W_{dc} = \frac{1}{2} C v_{dc}^2 \tag{4.3}$$

where v_{dc} is the dc-link voltage. If the losses of the actual converters can be considered to be small and thereby be neglected the energy in the dc-link capacitor depends upon the power, P_r, delivered to the rotor of the generator and the power, P_f, delivered to the grid filter as:

$$\frac{dW_{dc}}{dt} = \frac{1}{2} C \frac{dv_{dc}^2}{dt} = -P_r - P_f \tag{4.4}$$

One way of simplifying the control of the dc-link voltage is by utilizing feedback linearization, i.e., the nonlinear dynamics of the dc link are transformed into an equivalent linear system where linear control techniques can be applied. This can be done by letting $W = v_{dc}^2$, i.e.,

$$\frac{1}{2} C \frac{dW}{dt} = -P_r - P_f \tag{4.5}$$

Moreover, by letting the closed-loop current control dynamics be much faster than the closed-loop dc-link voltage dynamics the different time scales can be separated. This means that from the dc-link voltage controller point of view the rotor current can be considered to be identical to its reference value. Then the grid filter power can be expressed as $P_f = 3E_g i_{f,q}^{\text{ref}}$. The dc-link controller than acts on $i_{f,q}^{\text{ref}}$ as:

$$i_{f,q}^{\text{ref}} = k_p \cdot e_{dc} + k_i \int e_{dc} + G_a \cdot W$$
$$e_{dc} = W^{\text{ref}} - W \tag{4.6}$$

In the above control law the control gains are set according to:

$$k_p = -\frac{\alpha_{dc} C}{6E_{nom}} \qquad k_i = -0.01\frac{\alpha_{dc}^2 C}{6E_{nom}} \qquad G_a = 0.01\frac{\alpha_{dc} C}{6E_{nom}} \tag{4.7}$$

where α_{dc} is referred to as the bandwidth of the dc-link voltage controller.

4.3.3 Active and reactive power control loop

The active and reactive power of the wind turbine is controlled, in per-unit, by means of two individual PI controllers, as:

$$F(s) = k_p\left(1 + \frac{1}{T_i s}\right) = 5 \cdot \left(1 + \frac{1}{0.2 \cdot s}\right) \tag{4.8}$$

The active power control loop is acting on the *q* component of the rotor current reference while the reactive power control loop is acting on the *d* component of the rotor current.

To the active power reference a damping control term is added in order to provide additional damping to the drive train. The damping controller acts on the rotor speed (in per unit) and is a first order washout filter with a time constant of 0.5 s and a unity gain.

4.3.4 Rotor-current control loop

The rotor current is controlled by a P controller utilizing feed forward compensation as:

$$\mathbf{v}_R^{\text{ref}} = (\alpha_c L_\sigma)(\mathbf{i}_{\text{R}}^{\text{ref}} - \mathbf{i}_R) + j\omega_2 L_\sigma \mathbf{i}_R + \hat{\mathbf{E}} \tag{4.9}$$

In the above control law α_c is referred to as the bandwidth of the current control loop. The term $j\omega_2 L_\sigma \mathbf{i}_R$ is to remove the cross coupling between the *d* and *q* axis, and the term $\hat{\mathbf{E}}$ is an estimation of the back emf and is used as a feed-forward compensation.

4.3.5 Grid-filter current control loop

The grid filter current is controlled by a PI controller utilizing feed forward compensation as:

$$\begin{aligned} \mathbf{e}_f &= \mathbf{i}_f^{\text{ref}} - \mathbf{i}_f \\ \mathbf{v}_f^{\text{ref}} &= \left(\alpha_f L_l\right)\mathbf{e}_f + \left(\alpha_f R_f\right)\int \mathbf{e}_f dt + j\omega_1 L_f \mathbf{i}_f + \hat{\mathbf{E}} \end{aligned} \tag{4.10}$$

In the above control law α_f is referred to as the bandwidth of the grid filter current control loop and it is set to 2.0 pu. The term $j\omega_1 L_f \mathbf{i}_f$ is to remove the cross coupling between the *d* and *q* axis, and the term $\hat{\mathbf{E}}$ is an estimation of the back emf and is used as a feed-forward compensation.

5 Evaluation of risk for SSR in DFIG wind turbines

This chapter describes the adopted method for the evaluation of subsynchronous resonance in wind farms constituted by DFIG wind turbines. In order to simplify the investigation, the evaluation has been carried out by implementing an aggregated model of the wind farm, which is here constituted by one unique wind turbine. The adopted model for the DFIG system is the one described in the previous chapter. Simulation results for a DFIG-based wind farm radially connected to a series-compensated transmission line will be presented.

5.1 Introduction

In the previous chapter, the detailed model of the DFIG wind turbine, including the main parts of its control system, has been described. In this chapter, a wind farm constituted by DFIG-type wind turbines has been connected to a series-compensated transmission line in order to investigate the potential risk for SSR phenomena. The wind farm has been modeled as an aggregated wind turbine. In the specific case, the wind turbine is rated 2.6MW. Thus a special component available in the E-TRAN library for PSCAD/EMDC has been utilized to boost the output power of the system up to 890MW, in order to simulate the aggregated turbines.

In the following, the principle of the frequency scanning analysis, here utilized to estimate the harmonic impedance of the network, as well as the adopted method for the investigation will be discussed. Thus, the impact of the control system parameters on the risk for SSR conditions will be investigated through simulation results and then discussed.

5.2 Principle of frequency scanning analysis and implementation

Frequency scanning analysis [10,11] is a frequency method that can be used to screen system conditions that can give rise to potential resonances in the power network. The advantage of using this method is that it gives a quick and simple check to determine the system impedance seen from a specific bus at different frequencies.

A typical way to perform a frequency scanning, in order to estimate the harmonic impedance of the network seen from a specific bus, is to inject a harmonic current into the system and then measure the corresponding harmonic voltage.

In PSCAD/EMTDC, frequency scanning analysis can performed by using the "Harmonic impedance component", available in the Master Library of the

program and depicted in Fig. 18. When used, this component must be connected at the bus of interest.

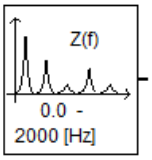

Fig. 18 - PSCAD harmonic impedance component.

Although very powerful, one drawback with this component is that it can only be used to calculate the impedance matrix of an electrical component. Components that are interfaced to EMTDC via a node-based electric interface (for example, an equivalent Norton current source, used when modeling an electrical machine) are not taken into account in the evaluation of the impedance matrix. Finally, this component cannot be used in case of user-written components. For these reasons, it is necessary to create a new component using FORTRAN language for this considered network model. Fig. 19 shows the aggregated wind turbine model with the PSCAD component utilized to perform the frequency scan. As shown, three controllable voltage sources have been connected to the point of common coupling (PCC) and both PCC voltages and currents are measured. Amplitude, phase and frequency of the applied voltages are calculated using the block "Harmonic Injection", visible in the figure, and added to the fundamental voltage. For each simulation, the frequency of the voltage is linearly increased from 0 Hz to 48 Hz in steps of 0.1 Hz and, when steady-state is reached, the harmonic impedance is evaluated from the knowledge of the harmonic voltage and the corresponding harmonic current.

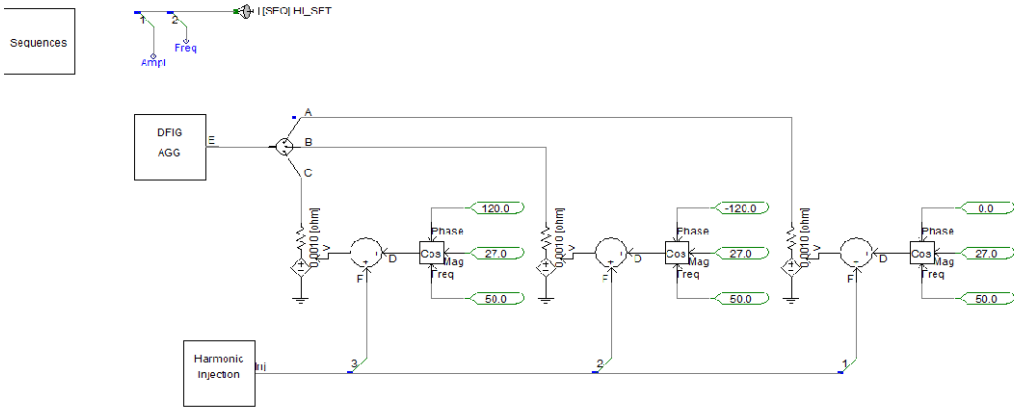

Fig. 19 - PSCAD print-screen of adopted method for harmonic impedance evaluation.

Different alternatives can be selected regarding the voltages to be applied. As an example, simulation programs such as PSS/E can only inject positive sequence components [33]. In such case, the voltages to be applied are calculated as:

$$\begin{aligned} Va\_FS_{(n)} &= V\sin(n\omega t) \\ Vb\_FS_{(n)} &= V\sin(n\omega t - 120^\circ) \\ Vc\_FS_{(n)} &= V\sin(n\omega t + 120^\circ) \end{aligned} \tag{5.1}$$

where *n* is the voltage harmonic order. This method can be used to investigate only positive-sequence harmonics, but does not give reliable results in case of other sequences (depending on the network configuration and on the installed components) or in case of inter-harmonics. The built-in PSCAD block in Fig. 18, instead, allows to separately calculate the three sequence impedances (positive-, negative- and zero-sequence components) separately.

If all sequence components are of interest in the investigation to be performed, the voltages to be applied by the controllable voltage sources should be calculated as [34,35]:

$$\begin{aligned} Va\_FS_{(n)} &= V\sin(n\omega t) \\ Vb\_FS_{(n)} &= V\sin\left[n(\omega t - 120^\circ)\right] \\ Vc\_FS_{(n)} &= V\sin\left[n(\omega t + 120^\circ)\right] \end{aligned} \tag{5.2}$$

Note that, as a difference compared with the set of equations in (5.1), the harmonic order *n* will affect not only the frequency of the voltage, but also the phase displacement. Therefore, if for example n=2, the phase of the voltage Vb_FS(2) will be -240°, while the phase of the voltage Vc_FS(2) will be +240°, meaning that the applied voltage is a negative sequence.

Although the method described by the set of equations (5.2) is more correct when investigating the harmonic behavior of a component/system in case of harmonic order higher than the fundamental, a different consideration must be made in case of subsynchronous voltages. This is mainly due to the fact that a three-phase subsynchronous voltage, as in the considered case, always rotates counterclockwise (positive direction), meaning that the subsynchronous voltage can always be seen as a positive-sequence component. To understand this, let us consider the generic case of a synchronous generator connected to a transmission line [36]. The interaction between the electrical and the mechanical system can be simulated by applying an oscillating speed ω to the generator shaft, as displayed in Fig. 20.

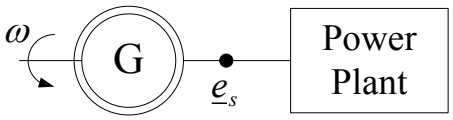

Fig. 20 - Simplified model of synchronous generator connected to transmission line for SSR studies.

The per-unit voltage at the generator terminals can be written in the $\alpha\beta$-plane as

$$\underline{e}_s^{(\alpha\beta)}(t) = e_{s,\alpha}(t) + je_{s,\beta}(t) = \bar{\omega}(t)E_s e^{j[\omega_0 t + \delta(t)]} \tag{5.3}$$

where $E(s)$ is the amplitude of the voltage vector at the generator terminals at rated speed, δ is its phase displacement, $\bar{\omega}$ is the per-unit rotor speed and ω_0 is the fundamental frequency expressed in rad/s. If the generator rotor oscillates around ω_0, its per-unit speed can be expressed as

$$\bar{\omega}(t) = \omega_0 + A\sin(\omega_m t) \tag{5.4}$$

where A is the amplitude of the oscillation and ω_m is the oscillation frequency (in rad/s) of the rotor. Substituting (5.4) in (5.3), the α-component of the output voltage can be written as

$$\begin{aligned} e_{s,\alpha}(t) = [\bar{\omega}_0 + A\sin(\omega_m t)]E_s\cos[\omega_0 t + \delta(t)] \\ = \bar{\omega}_0 E_s\cos[\omega_0 t + \delta(t)] \\ + \frac{AE_s}{2}\{-\sin[(\omega_0 - \omega_m)t + \delta(t)] \\ + \sin[(\omega_0 + \omega_m)t + \delta(t)]\} \end{aligned} \tag{5.5}$$

The derivative of the rotor angle δ is given by

$$\frac{d\delta(t)}{dt} = [\bar{\omega}(t) - \omega_0]\omega_B = A\sin(\omega_m t)\omega_B \tag{5.6}$$

with ω_B the base frequency in rad/s. Therefore, by integrating both sides of (5.6) and calling δ_0 the rotor angle in steady-state conditions, the rotor angle can be expressed as

$$\delta(t) = \delta_0 - A\frac{\omega_B}{\omega_m}\cos(\omega_m t) \tag{5.7}$$

Substituting (5.7) in (5.5) and after some algebraic manipulations, the α-component of the voltage output of the generator is given by

$$\begin{aligned} e_{s,\alpha}(t) = \bar{\omega}_0 E_s \cos(\omega_0 t + \delta_0) \\ + \frac{AE_s}{2\omega_m}\{(\omega_0 \\ - \omega_m)\sin[(\omega_0 - \omega_m)t + \delta_0] + (\omega_0 \\ + \omega_m)\sin[(\omega_0 + \omega_m)t + \delta_0]\} \end{aligned} \tag{5.8}$$

Analogously, the β-component of the voltage is found to be equal to

$$\begin{aligned} e_{s,\beta}(t) = \bar{\omega}_0 E_s \sin(\omega_0 t + \delta_0) + \frac{AE_s}{2\omega_m}\{-(\omega_0 \\ - \omega_m)\cos[(\omega_0 - \omega_m)t + \delta_0] - (\omega_0 \\ + \omega_m)\cos[(\omega_0 + \omega_m)t + \delta_0]\} \end{aligned} \tag{5.9}$$

As shown in (5.8) and (5.9), when a small oscillation is applied to the generator rotor, the output voltage will be constituted by the sum of three terms: one term rotating at the rated frequency plus two terms oscillating with frequencies of $\omega_0 + \omega_m$, corresponding to the supersynchronous voltage component, and $\omega_0 - \omega_m$, corresponding to the subsynchronous component. It is of interest to observe that the amplitude of the supersynchronous component is higher as compared with the subsynchronous one. However, the network usually presents a small positive damping at these frequencies [11], thus the supersynchronous voltage does not represent a risk for the power plant. Being the focus of this report, let us consider the subsynchronous component of the voltage only. From (5.8) and (5.9), the subsynchronous component of the measured voltage is given by

$$\begin{aligned} \underline{e}_{s,sub}^{(\alpha\beta)}(t) = \frac{AE_s}{2\omega_m}(\omega_0 \\ - \omega_m)\{\sin[(\omega_0 - \omega_m)t + \delta_0] \\ + j\cos[(\omega_0 - \omega_m)t + \delta_0]\} \\ = -\frac{AE_s}{2\omega_m}(\omega_0 - \omega_m)e^{j[(\omega_0 - \omega_m)t + \delta_0 + \pi/2]} \end{aligned} \tag{5.10}$$

meaning that the subsynchronous voltage vector rotates in the positive direction (counterclockwise) in the $\alpha\beta$-plane (thus, in the three-phase system). Observe that the obtained result is valid independently on the applied oscillating frequency ω_m.

The voltage vector $\underline{e}_s^{(\alpha\beta)}$ can be further transformed in the synchronous reference plane as

$$\underline{e}_s^{(dq)}(t) = \underline{e}_s^{(\alpha\beta)}(t)e^{-j\omega_0 t} = \underline{e}_{s,f}^{(dq)}(t) + \underline{e}_{s,sub}^{(dq)}(t) \tag{5.11}$$

where $\underline{e}_{s,f}^{(dq)}$ is the *dq*-voltage vector at the fundamental frequency. The subsynchronous voltage component is given by

$$\underline{e}_{s,sub}^{(dq)}(t) = \underline{e}_{s,sub}^{(\alpha\beta)}(t)e^{-j\omega_0 t} = -\frac{AE_s}{2\omega_m}(\omega_0 - \omega_m)e^{-j(\omega_m t + \delta_0 + \pi/2)} \tag{5.12}$$

From (5.12) it can be observed that although the subsynchronous component of the voltage $\underline{e}_{s,sub}^{(\alpha\beta)}$ rotates in the positive direction in the fixed $\alpha\beta$-plane, the same vector rotates clockwise in the *dq*-plane that rotates synchronously with the rated frequency of the system, thus it can be treated as a negative-sequence component. This is of high importance when performing SSR analysis using frequency scanning technique or when deriving a SSR damping controller.

5.3 Principle of SSR in DFIG-based wind turbine

In order to understand the principle that leads to SSR between a DFIG-based wind farm and a series-compensated network, it is of importance to consider that, being a controlled power source, at different frequencies the wind turbine can be seen as a controllable impedance. This approach is similar to the one utilized for example for HVDC systems and typically addressed to as input admittance [19,20]. If the real part of the controllable impedance is negative (negative resistance) for a given frequency, the wind turbine is injecting active power in the network. The wind turbine is absorbing active power from the network otherwise. Similar analogy can be made for the correspondence between the imaginary part of the controllable impedance (reactance) and the reactive power exchanged between the network and the wind turbine. If the imaginary part of the controllable impedance crosses the zero, it denotes a resonant condition at the specific frequency.

It is of importance to underline that the parameters of this impedance (thus its resonant frequency) depend on several parameters, such as the base quantities of the induction generator and, for a given machine, the controller settings. As an example, the harmonic impedance obtained from the frequency scan of a 2.6MW DFIG wind turbine is depicted in Fig. 21. The frequency of the subsynchronous component in the applied voltage (see previous section) is varied from 0 to 48 Hz in steps of 0.1 Hz, while the amplitude of the subsynchronous voltage is set equal to 0.02 pu. The power out of the turbine is set to 0.9 pu. Here, for clarity of the analysis, the DFIG system has been simplified and it is assumed that the dc-link capacitors for the back-to-back converter are infinitely large (this is achieved by connecting an ideal dc voltage source to the dc-link of the rotor-side converter). As a result, only the control system for the rotor-side converter can impact the harmonic impedance of the turbine.

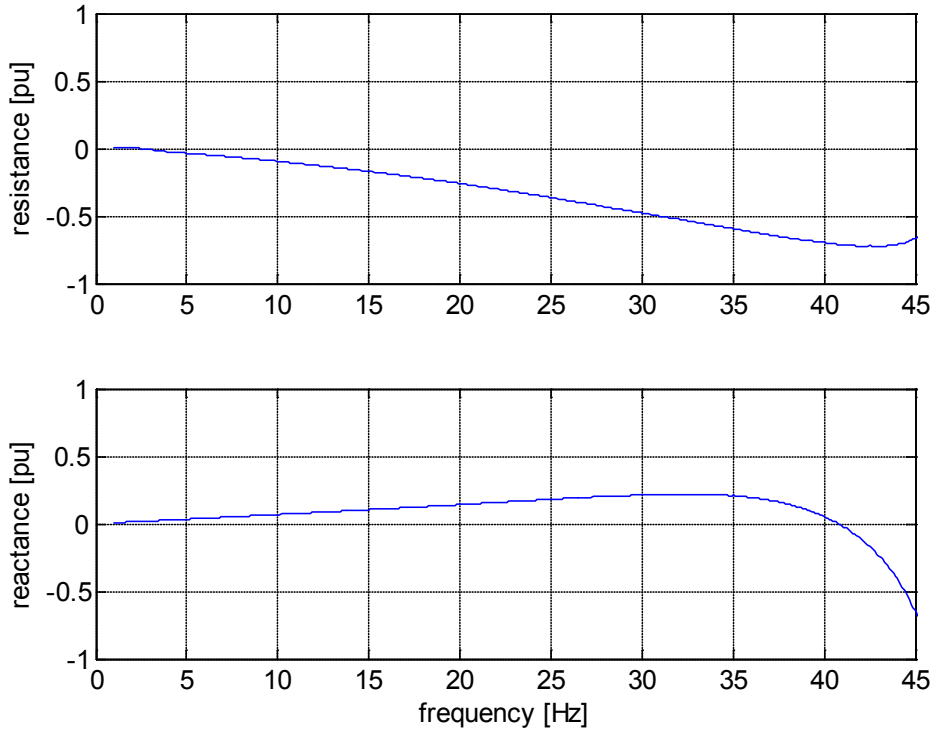

Fig. 21 - Trend of DFIG harmonic impedance (real and imaginary part) as a function of the modulation frequency. Output power equal to 0.9pu.

From the plot, it is clearly visible that the harmonic resistance of the turbine for frequencies below the fundamental is negative. Furthermore, the harmonic reactance of the turbine presents a zero-crossing around 41Hz, denoting that at this frequency the wind turbine presents a resonant condition. If a matching resonant frequency exists in the transmission network, due to the series compensation, an SSR might be experienced. This is exemplified in Fig. 22. An unstable oscillation will be triggered if the sum of the equivalent resistance of the wind turbine and the network resistance at the frequency of interest is less than zero (total negative resistance).

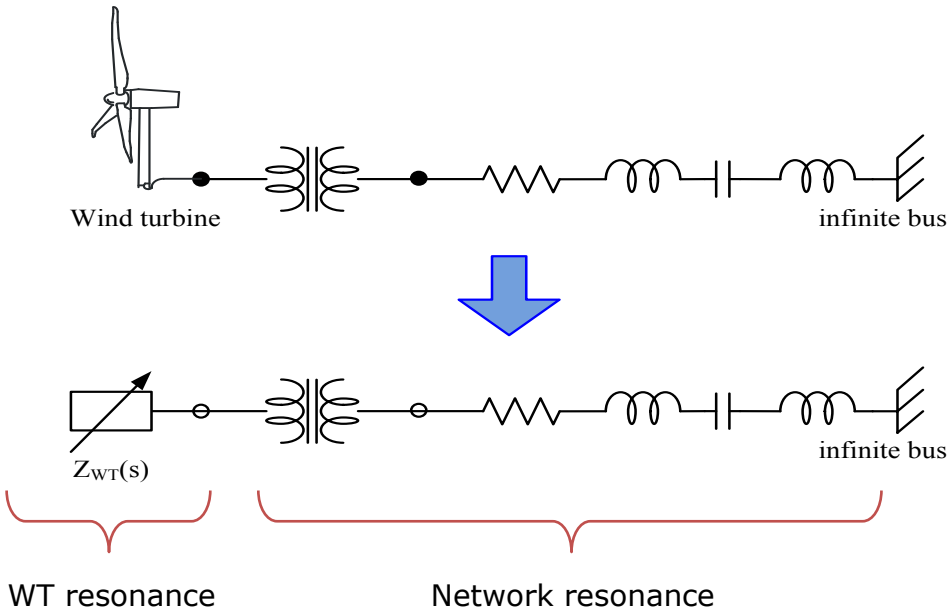

Fig. 22 - Top: wind turbine (or aggregated wind farm) radially connected to series-compensated tranmission system. Bottom: principle of SSR formation: an SSR might be triggered if the resonance frequency of the wind turbine matches the resonance frequency of the network.

As already mentioned earlier in this chapter, the trend of the equivalent impedance for the wind turbine as a function of the frequency depends on the wind turbine controller settings.
In the following, the impact of different parts of the control system for the DFIG (rotor current controller, dc-link voltage controller, phase-locked loop) will be investigated. Furthermore, the impact of the operating conditions of the system on the risk of SSR will be discussed.

5.4 SSR risk evaluation

This section presents the obtained simulation results for the evaluation of the risk of SSR for DFIG-based wind farm radially connected to a series-compensated transmission network. To perform this evaluation, the model depicted in Fig. 23 has been implemented in the simulation tool PSCAD/EMTDC. The control system for the DFIG is the one described in Chapter 4. As shown in the figure, the aggregated model of the wind farm, described earlier in this report, is connected to a 539 kV transmission network trough a step-up transformer (same voltage level as the one utilized for the first benchmark model on SSR developed by IEEE). The transmission network is constituted by two 100 km lines connected in parallel: one line is uncompensated and directly connected to an infinite bus, while the other line is series compensated. The series compensation level can be varied through a slider visible in Fig. 23. At a given time instant, controlled by the user, the circuit breaker BRK_SC can be opened, letting the wind farm be radially connected to the series-compensated line; this would resemble a system

configuration similar to the one that led to the event in the Zorillo Gulf Wind Farms in Texas.

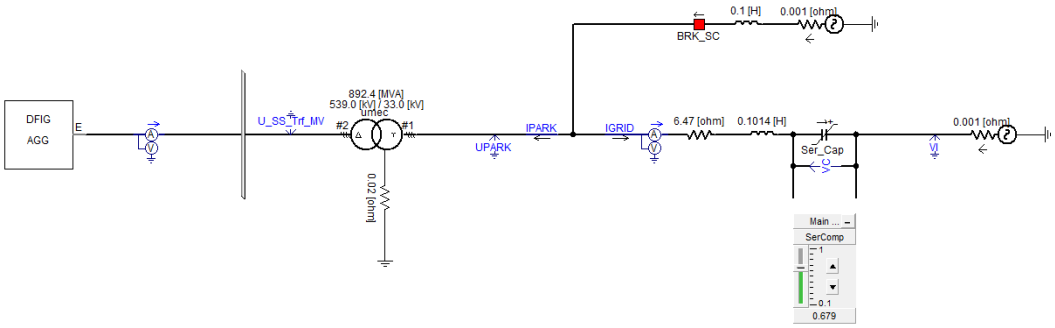

Fig. 23 - PSCAD/EMTDC print screen of simulated system. The series-compensation level can be adjusted online.

In the following, the obtained simulation results will be shown. In particular, the impact of the control settings for the DFIG wind turbine on the risk for SSR will be described.

5.4.1 Impact of rotor current controller bandwidth

At first, the impact of the rotor-side current controller on the harmonic impedance of the DFIG system will be investigated. To analyze the impact of the current controller only, it is assumed that an ideal dc source is connected to the dc side of the rotor converter (see Section 5.3). The grid-side converter is disconnected from the mains. The resulting harmonic impedance from the DFIG system is depicted in Fig. 21, while Fig. 24 shows the impact of the current controller bandwidth on the DFIG harmonic impedance. The bandwidth of the PLL is set equal to 0.1 pu. It is of interest to observe that when increasing the bandwidth α_{cc}, the resonant frequency of the DFIG system moves toward higher frequencies while the equivalent negative resistance becomes more negative. This is summarized in Fig. 25; note that a variation of the controller bandwidth from 2 pu to 10 pu leads to a variation of the resonant frequency of the DFIG system of about 2 Hz.

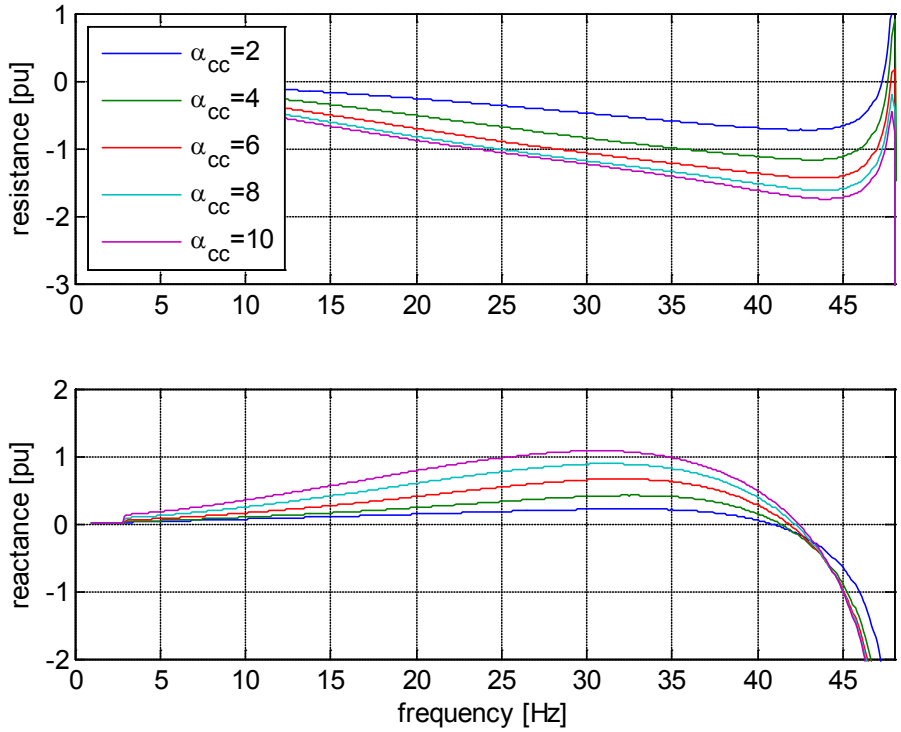

Fig. 24 - Trend of DFIG harmonic impedance (real and imaginary part) as a function of the modulation frequency. Infinite dc source connected to the dc side of rotor converter. Grid-side converter disconnected. Current controller bandwidth (α_{cc}) varied from 2 pu to 10 pu in steps of 2 pu. Output power equal to 0.9pu.

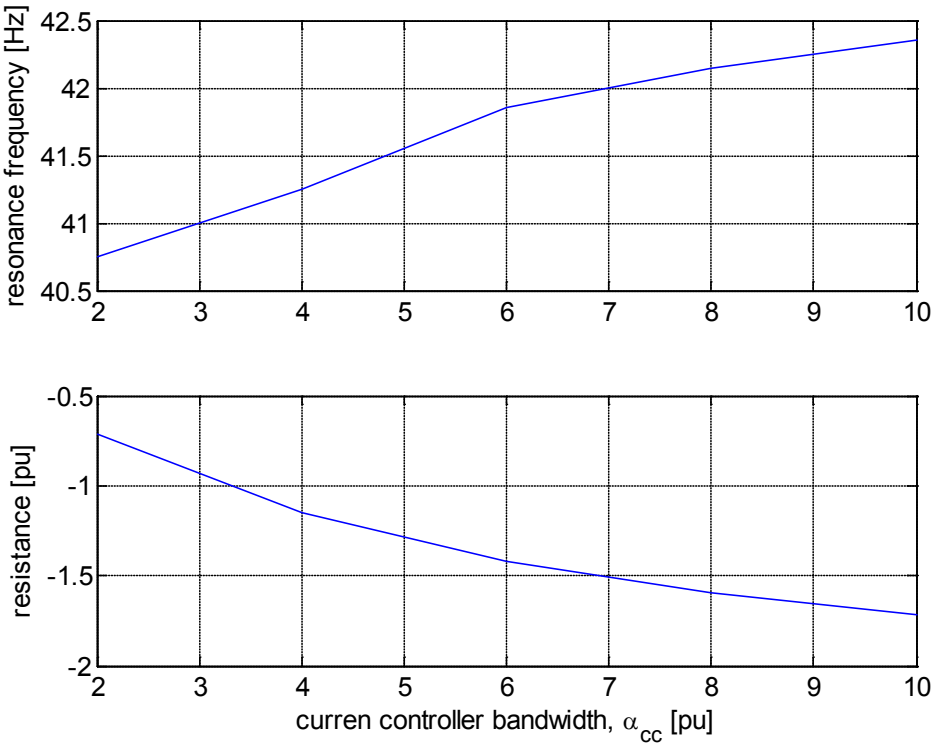

Fig. 25 - Trend of DFIG resonance frequency (top) and corresponding equivalent resistance (bottom) as a function of the current controller bandwidth. Ideal dc source case. Output power equal to 0.9pu.

For the results shown above, it has been assumed that the time constant of the dc storage for the back-to-back converter of the DFIG system is infinitely large, meaning that the grid-side converter was not included in the investigation. Fig. 26 and Fig. 27 show instead the trend of the harmonic impedance of the DFIG and the corresponding resonance frequency and equivalent resistance when varying the rotor current controller bandwidth under the realistic case of a finite energy storage mounted on the dc side of the converter. For proper comparison, as in the previous case the power output of the wind turbine is set to 0.9 pu. The bandwidth of the dc-link voltage controller is set to 0.2 pu, i.e. ten times below the lowest considered bandwidth of the rotor current controller. This selection has been made to guarantee the stability of the control system. Observe that the impact of the dc-link controller (together with the filters of the grid-side converter) is to move the resonant frequencies up in range. More interesting is to compare the latter results with the one obtained in the case of ideal dc source. From Fig. 28 it can be observed that the dc-link voltage controller has a beneficial impact on the equivalent resistance of the machine, which now is less negative as compared with the case of an ideal dc source. This is mainly due to the fact that the machine is operating at supersynchronous speed (power output is equal to 0.9 pu), meaning that the grid-side converter is operating as an inverter, i.e. it injects power into the ac network. As reported in [19],

under these conditions the control system adds damping to the electrical system in the subsynchronous range.

If the power output of the DFIG is lowered to 0.2 pu (see Fig. 29, where the relation between output power and rotor speed is depicted), meaning that the grid-side converter will operate as a rectifier, the equivalent resistance (thus, the damping introduced by the dc-link voltage controller in the network) will be lowered. This is clearly visible in Fig. 30, where the comparison between the trend of the DFIG resonance frequency and the corresponding equivalent resistance as a function of the current controller bandwidth in case of 0.9 pu (blue curve) and 0.2 pu (red curve) power output is shown. From the figure it can also be concluded that the resonant frequency of the DFIG is a function of the operating point, i.e. of the amount of power that the wind turbine is injecting into the grid. The latter results are summarized in the plot in Fig. 31, where the trend of DFIG resonance frequency (top) and corresponding equivalent resistance (bottom) as a function of the output power are shown. For this set of results, the bandwidth of the rotor current controller, α_{cc}, is set equal to 2 pu and the power out of the turbine is varied from 0.05 to 0.9 pu in steps of 0.05 pu. As expected, at low wind speeds, i.e. when the active power out of the turbine is low, the DFIG presents a large negative resistance which varies considerably with the output power. Observe that for output power higher than 0.3 pu, i.e. when the rotor speed is constant and higher than the synchronous speed, the variation of the DFIG resistance is lower as compared with the subsynchronous operations.

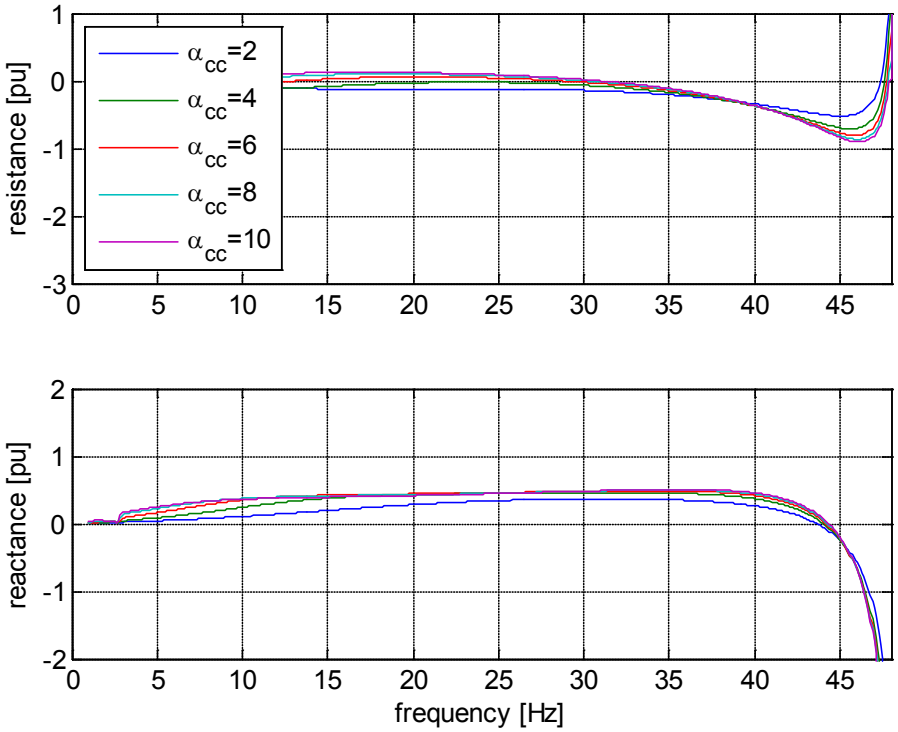

Fig. 26 - Trend of DFIG harmonic impedance (real and imaginary part) as a function of the modulation frequency. Dc-link of back-to-back converter controlled through the grid-side converter. Current controller bandwidth (α_{cc}) varied from 2 pu to 10 pu in steps of 2 pu. Output power equal to 0.9pu.

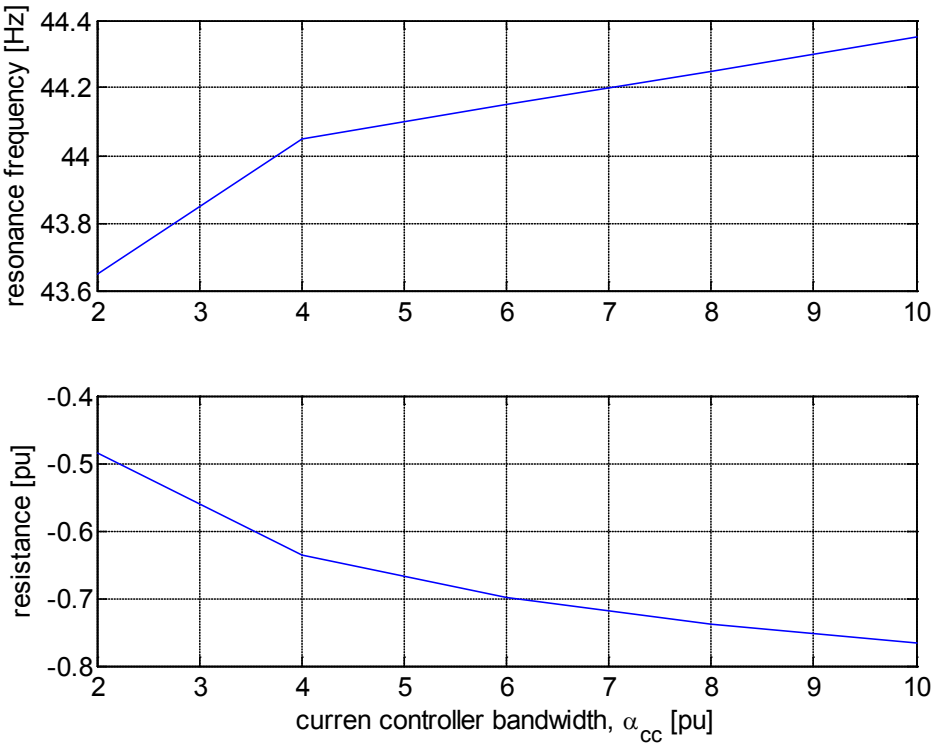

Fig. 27 - Trend of DFIG resonance frequency (top) and corresponding equivalent resistance (bottom) as a function of the current controller bandwidth. Dc-link of back-to-back converter controlled through the grid-side converter. Output power equal to 0.9pu.

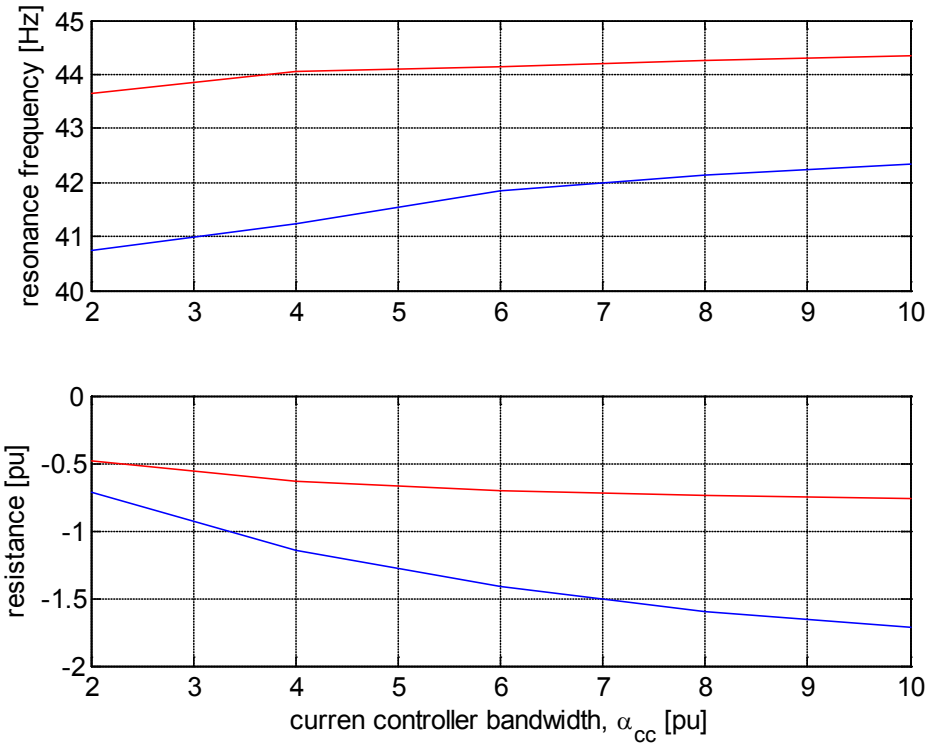

Fig. 28 - Trend of DFIG resonance frequency (top) and corresponding equivalent resistance (bottom) as a function of the current controller bandwidth. Comparison between ideal dc source case (blue curve) and actual configuration (red curve). Output power equal to 0.9pu.

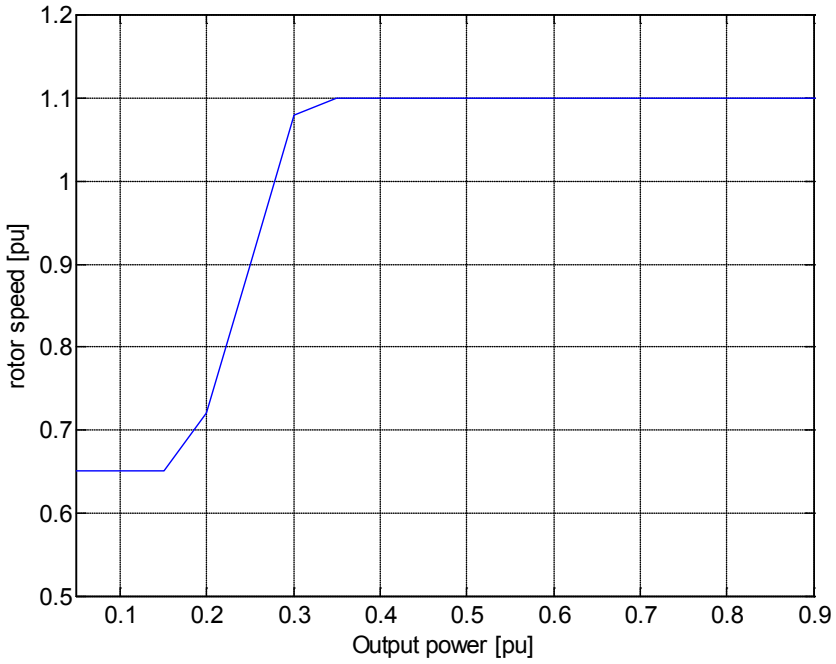

Fig. 29 – Relation between rotor speed and output power.

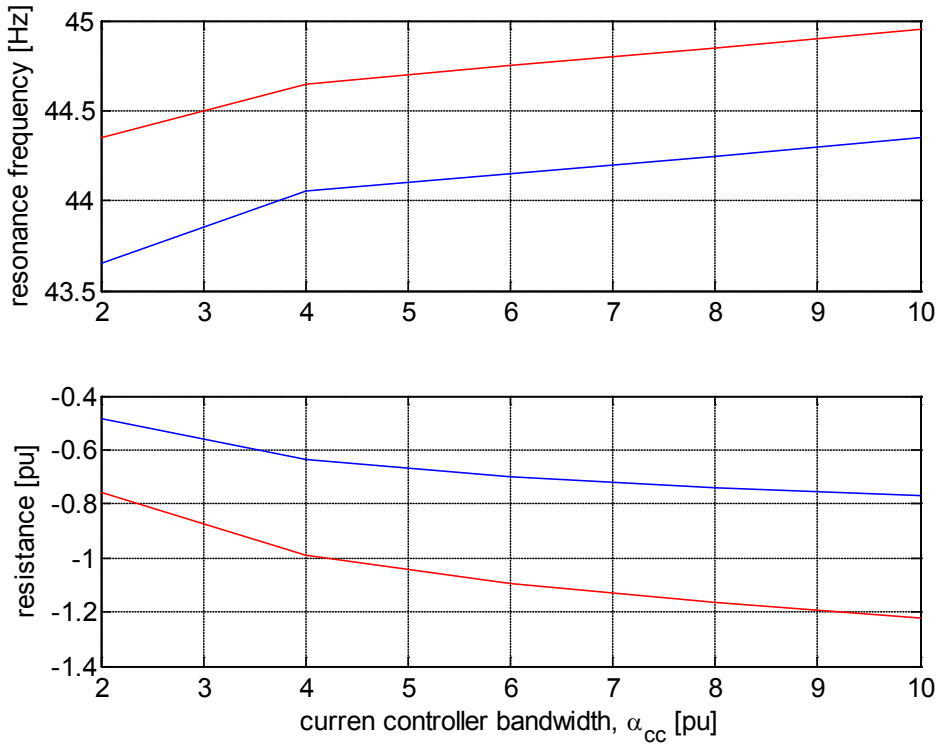

Fig. 30 - Trend of DFIG resonance frequency (top) and corresponding equivalent resistance (bottom) as a function of the current controller bandwidth. Blue curve: output power equal to 0.9 pu; red curve: output power equal to 0.2 pu.

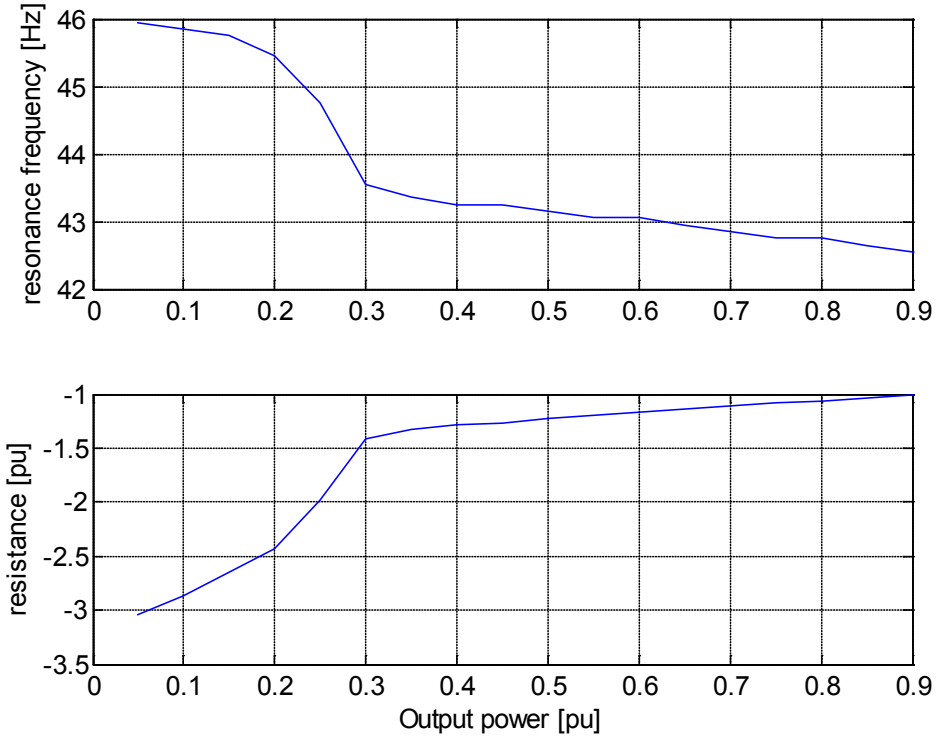

Fig. 31 - Trend of DFIG resonance frequency (top) and corresponding equivalent resistance (bottom) as a function of the DFIG output power. Dc-link of back-to-back converter controlled through the grid-side converter. Current controller bandwidth equal to 2 pu.

When connected to the transmission system, an oscillatory condition can be triggered if a matching frequency exists. As an example, here the series compensation level has been set to 68% of the line impedance, resulting in a resonant frequency for the series-compensated line of 41.2 Hz. Fig. 32 shows the transmitted active power directly after the opening of the circuit breaker BRK_SC in Fig. 23 when different bandwidths for the rotor current controller are used. Observe that (also in agreement with the results in Fig. 25) when α_{cc}=2pu there is a perfect match between the resonant frequency for the DFIG and the network resonance. As a result, sustained oscillations will be experienced in the system. Due to the match in frequency and to the low amount of resistance (thus, damping), in the modeled network, these oscillations will grow very fast. Increasing the controller bandwidth to 4pu will improve the situation, since there is not a perfect match between the two resonances. Even, if the system appears more damped as compared with the previous case it will still result unstable, since the resonance is still very close. In order to ensure stable operation of the system for the specific simulated case, the bandwidth of the rotor current controller must be increased even further (here has been set to 10 pu) and the dc-link voltage controller must be activated. In this way, as it can also be seen from Fig. 27 and Fig. 28, the resonance frequency for the DFIG goes up to 44.9 Hz, which is outside the

resonant frequency range of the network. As a result the system will manage to reach steady state after some oscillations.

Observe that, in order to emphasize the impact of the controller on the investigated phenomenon, all protections in the DFIG model are disabled. The same condition holds for the results obtained in the following sections.

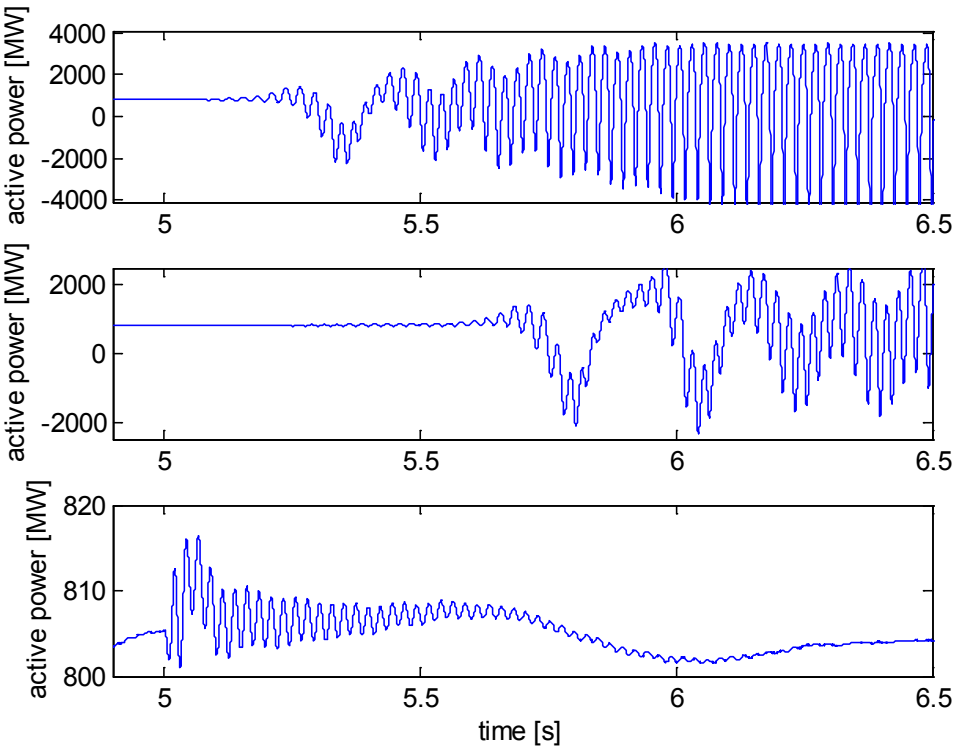

Fig. 32 - Transmitted active power after line disconnection. Series compensation level equal to 68%. Top: α_{cc} =2 pu, ideal dc source case; middle: α_{cc} =4 pu, ideal dc source case; bottom: α_{cc} =10 pu, actual configuration. Output power equal to 0.9pu.

5.4.2 Impact of dc-link voltage controller bandwidth

From the simulation results presented in the previous section, it has been shown that the rotor-side current controller has an impact on the equivalent harmonic impedance of the DFIG system. Furthermore, it has been demonstrated that the presence of the dc-link voltage controller as well as the point of operation has a major impact on the resonant condition of the system. For this reason, it can be of interest to investigate the impact of the dc-link voltage controller bandwidth (α_{dc}) on the DFIG harmonic impedance. For the results depicted in Fig. 33, the α_{dc} has been changed from 0.1 pu to 0.4 pu for the two extreme conditions of the current controller bandwidth. The PLL bandwidth is left unchanged and equal to 0.1 pu. For all considered cases, the power output of the wind turbine is 0.9 pu. Observe that the variation of

the dc-link controller bandwidth has very little impact on the overall DFIG harmonic impedance.

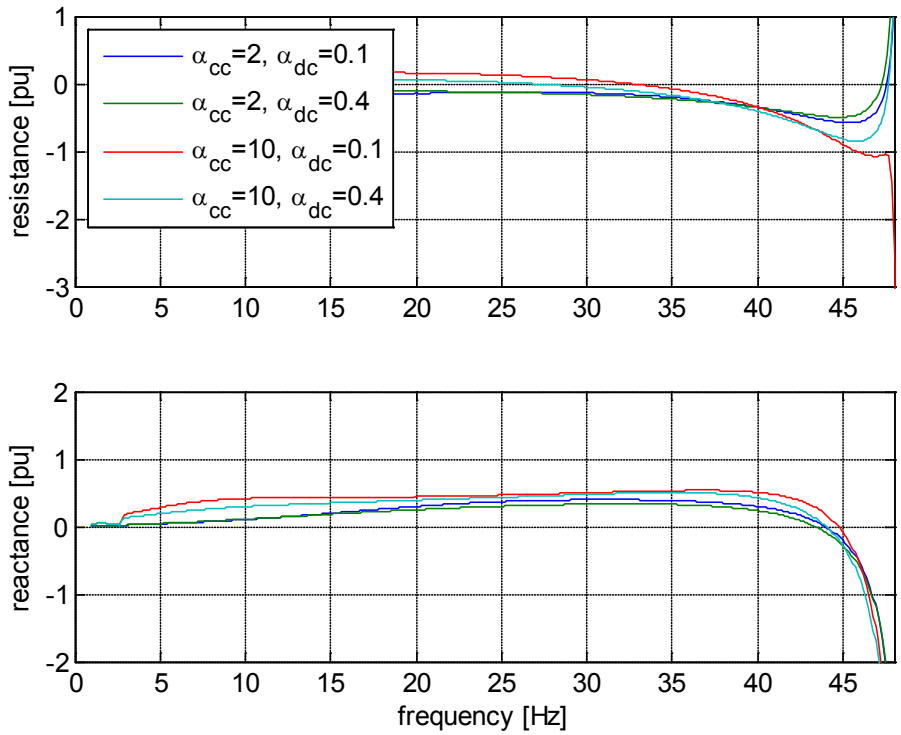

Fig. 33 - Trend of DFIG harmonic impedance (real and imaginary part) as a function of the modulation frequency. Impact of current controller bandwidth (α_{cc}) and dc-link voltage controller bandwidth (α_{dc}).

5.4.3 Impact of reactive power controller bandwidth

As explained in Section 4.3.3, the reference currents for the rotor-side current controller are calculated through an active and a reactive power control loop. Typically, both the active and the reactive power controllers are characterized by low bandwidth, in order to increase the stability margin of the overall control system. However, in some countries the wind turbine/farm can be involved in the reactive power support to the network. In such a case, the speed of response of the reactive power controller can be increased to higher values. For this reason, it can be of interest to investigate the impact of the reactive power controller of the harmonic impedance of the DFIG system. Fig. 34 shows the trend of DFIG resonance frequency (top) and corresponding equivalent resistance (bottom) as a function of the reactive power controller bandwidth. For this set of simulations, the proportional gain of the reactive power controller has been varied from 1 to 7 pu in steps of 1 pu, while the integrator time constant, see (4.8), has been kept constant to 0.2 s. The current controller bandwidth is equal to 2 pu, while the dc-link voltage controller has a bandwidth of 0.2 pu. Observe that the parameters for the

active power controllers are kept to K_p=5 pu and T_i=0.2 s, has described in (4.8). The measured active power sent to the control system is passed through a low-pass filter having a time constant of 0.2 s. The presence of this will limit the overall bandwidth of this control loop.

From the figure blow it can be observed that the reactive power controller mainly impacts the resonance frequency of the DFIG harmonic impedance, while it has an almost negligible impact on the damping.

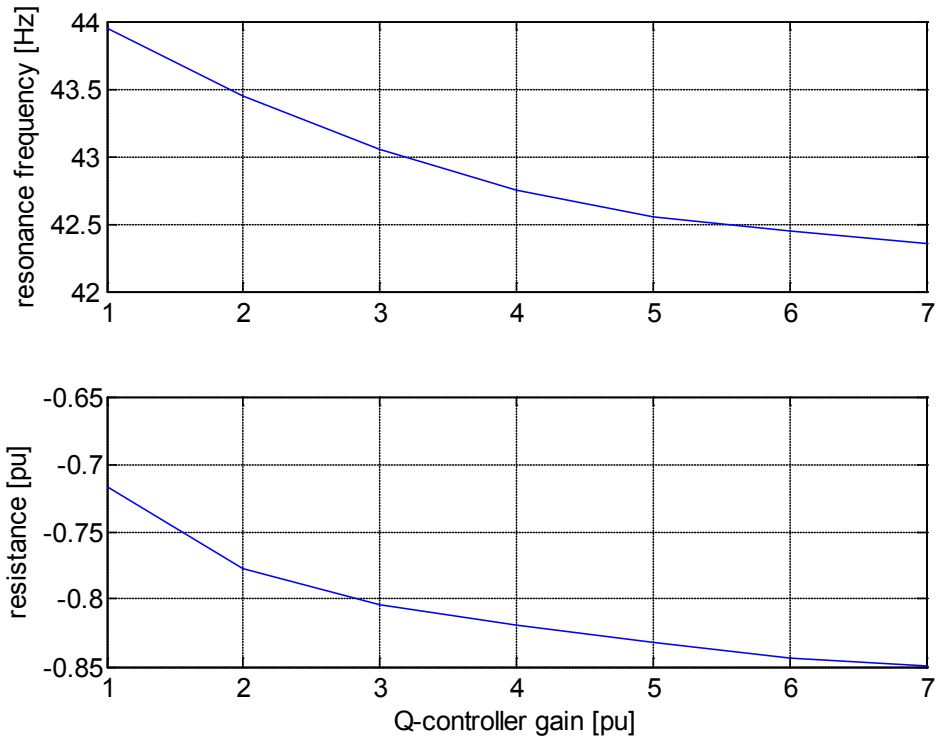

Fig. 34 - Trend of DFIG resonance frequency (top) and corresponding equivalent resistance (bottom) as a function of the reactive power controller bandwidth.

5.4.4 Impact of PLL bandwidth

As explained in Chapter 4, the control system of the DFIG turbine is implemented in the rotating *dq*-coordinate system and the needed transformation angle is obtained through a PLL. Although not often considered when describing a control algorithm, the PLL plays an important role in the overall control structure. Fig. 35 shows the impact of the PLL bandwidth (α_{PLL}) on the DFIG harmonic impedance. Similar to the results presented in Fig. 33, α_{PLL} has been varied (in this case from 0.01 pu to 0.2 pu) for the two extreme conditions of the current controller bandwidth. Again, the power output of the wind turbine is 0.9 pu. As expected, the variation of the PLL bandwidth has a fairly large impact on the overall DFIG harmonic impedance. This is mainly

due to the ability of the control system to "see" the oscillatory component in the measured signal due to the SSR and counteract.

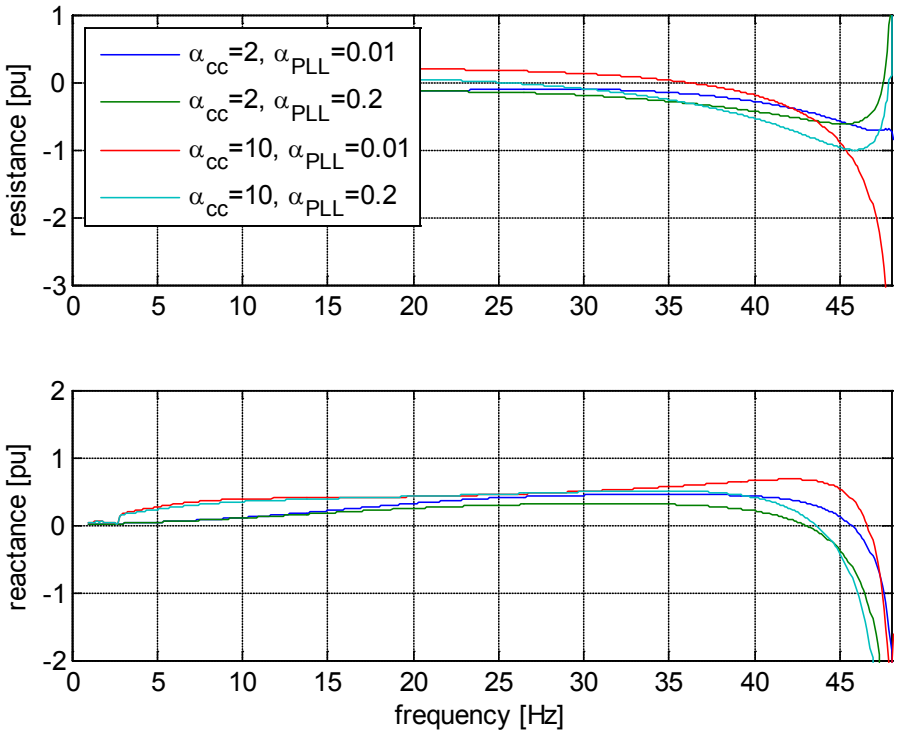

Fig. 35 - Trend of DFIG harmonic impedance (real and imaginary part) as a function of the modulation frequency. Impact of current controller bandwidth (α_{cc}) and PLL bandwidth (α_{PLL}).

5.5 Conclusions

In this chapter, the adopted method for the evaluation of subsynchronous resonance in wind farms constituted by DFIG wind turbines has been explained. The model considered is a wind farm constituted by DFIG-type wind turbines radially connected to a series-compensated transmission line.
At first, the principle of the frequency scanning analysis, utilized to estimate the harmonic impedance of the system, as well as the adopted method for the investigation has been discussed. Thus, the control system parameters that might impact on the condition for a SSR have been investigated through simulation results. It has been shown that both the current controller and the phase-locked loop have a major impact on the harmonic impedance (thus on the risk for SSR conditions) of the DFIG system, while the system seems to be less sensitive to variations of the dc-link voltage controller bandwidth. Furthermore, as anticipated, the point of operation of the wind turbine, i.e. the amount of power output of the turbine, will also impact the characteristic frequency of the DFIG system.

6 Conclusions and Future work

6.1 Conclusions

This report has dealt with the investigation of potential risk for subsynchronous resonance (SSR) in case of wind farms connected to series-compensated transmission lines. As first, Chapter 2 gave an overview of the problem of SSR in power systems. Definition as well as classification of different kind of SSR that can be encountered in the power systems has been given. Analysis methods to investigate the risk for SSR and possible countermeasures available in the market have been briefly discussed in this chapter.

In Chapter 3, an overview of the risk for SSR conditions in case of wind farms connected to series-compensated transmission lines has been given. The three main turbine topologies (fixed speed, full-power converter and doubly-fed induction generator, DFIG, type), have been briefly described and for all of them the potential risk for SSR has been discussed. As mentioned, fixed speed wind turbines might be affected by SSR when radially connected to a series compensated line, while variable-speed full power converter turbines seems to be immune to the phenomena, thanks to the decoupling between the generator and the transmission line offered by the converter. The latter consideration also holds for wind farms connected to the power systems through HVDC systems.

Different scenarios appear for the DFIG type. This variable-speed turbine was the one employed the first incident that has been registered and identified as SSR. For this reason, the focus of Chapters 4 and 5 has been on this turbine topology. In particular, the modeling of the DFIG system together with the control strategy adopted for this report is described in Chapter 4. Then, in Chapter 5 the adopted method for the evaluation of subsynchronous resonance in wind farms with DFIG wind turbines has been explained. The model here considered is a wind farm constituted by DFIG wind turbines radially connected to a series-compensated transmission line. As first, the principle of the frequency scanning analysis, utilized to estimate the harmonic impedance of the network, as well as the adopted method for the investigation has been discussed. Thus, the impact of the control system parameters on possible SSR conditions has been investigated through simulation results. It has been shown that both the current controller and the phase-locked loop have a major impact on the harmonic impedance (thus on the risk for SSR conditions) of the DFIG system, while the system seems to be less sensitive to variations of the dc-link voltage controller bandwidth. Furthermore, the point of operation of the wind turbine, i.e. the amount of power output of the turbine, will also impact the characteristic frequency of the DFIG system. This is mainly due to the different operation of the grid-side converter as a function of the power out of the turbine.

Another important conclusion is that resonant conditions between the wind farm and the turbine can occur for a fairly wide frequency range (up to a few Hz), i.e. for a wide range of series compensation level. This is identified as

one of the major differences as compared with SSR in case of synchronous generators. In the latter case, SSR are mainly due to TI; since for this kind of SSR the natural frequencies of the turbine-generator shaft system are involved, the resonant frequencies are typically fixed and well known. Furthermore, the mechanical frequencies are very sharp. This results in an easier approach when trying to provide extra damping by aims, for example, of a FACTS controller.

6.2 Future Work

The results obtained throughout this investigation have clearly shown that there is a potential risk for SSR in wind farms connected to series compensated transmission lines. Furthermore, this work has served as a basis to identify possible future activities within this field. These are summarized below:

- Due to the limited time available, the investigation performed in this report was mainly based on the frequency scanning approach. Although effective, this method can only give an indication of the risk for an SSR condition and has to be validated through time domain simulations. Although more cumbersome, a more mathematical approach, maybe based on the input-admittance passivity as the one utilized for the HVDC system and presented in [19,20] can lead to more accurate results. Furthermore, a mathematical approach can facilitate the system sensitivity analysis.
- In order to facilitate the understanding of the conditions that might lead to a SSR condition in a wind farm, the farm as been aggregated into one single wind turbine. Although this approach is often used and was considered acceptable for this pre-study, it can be of high interest to model a wind farm with a significant amount of turbines and to investigate the impact of the temporal and spatial distribution of instantaneous wind speed on the susceptibility of plant to trigger SSR
- It has been shown that the frequency range where an unstable oscillation can be triggered is fairly large and is mainly dependent on the controller parameters settings. If a mathematical approach is decided (as suggested in the previous point), it can be of interest to identify possible suggestions for the selection of the controllers in order to avoid/limit SSR conditions.
- The investigated network deals with radial resonance. This choice was made to resemble the condition that has led to the event in Zorillo. Furthermore, a radial resonance leads to a fairly deep negative undamping. For this reason, radial resistance is generally considered the most dangerous condition. However, it could be of interest to investigate other kind of resonant conditions, such as parallel resonance. Although less severe than the radial one, one characteristic of the parallel resonance is that the frequency range where the network exhibits a negative damping is wider as compared with the radial case. This could be of high importance for the specific case of SSR in wind turbines.

- The back-to-back converter available in a DFIG system can be used to provide extra damping in case of a resonant condition. This seems to be possible thanks to the relatively low frequency of these oscillations as compared, for example, with the bandwidth of the current controllers. The investigation as well as the implementation of such a damping controller can be of high interest and might relive the wind farm owner from the installation of an expensive additional damping device (for example, a blocking filter or a FACTS controller).
- In some cases, due to the wide frequency range where a resonant condition might occur, it might be necessary with the installation of an additional device. As already mentioned in Section 2.4.3, FACTS controllers are today considered a valuable solution for SSR mitigation. Furthermore, these kind of devices are already employed in wind farms for other reasons and it can be cost-effective to add extra damping functionalities to this kind of devices. However, one major difference as compared with SSR in synchronous generators is that the characteristic frequency of these oscillations is not fixed (is not related to the mechanical resonance). For this reason, the investigation and implementation of optimal control algorithms for the specific purpose of SSR damping in wind farms will be a challenge.

7 References

[1] T. Ackerman, Wind power in power systems, New York: Wiley, 2005.

[2] Anaya Lara, Jenkins, Ekanayake, Cartwright, Huges, Wind Energy Generation Modeling and Control, United Kingdom: Wiley, 2009.

[3] P. Pourbeik, R.J. Koessler, D.L. Dickmander, W. Wong, "Integration of large wind farms into utility grids (part 2 performance issues)", *Power Engineering Society General Meeting, 2003, IEEE* , vol. 3, pp. 1520-1525, 13-17 July 2003.

[4] "Large-Scale Wind Integration Studies in the United States: Preliminary Results," *NREL/CP-550-46527, Sep. 2009.* [online]. Available: www.nrel.gov

[5] "Global Wind Energy Outlook 2010," [online]. Available: www.gwec.net

[6] "Southern Alberta Transmission Reinforcement Needs Identification Document," [online]. Available: http://www.aeso.ca

[7] M. Henderson, D. Bertagnolli, D. Ramey, "Planning HVDC and FACTS in New England," *IEEE/PES Power Systems Conference and Exposition, 2009, PSCE '09.* pp. 1-3, 15-18 Mar. 2009.

[8] "Ercot CREZ Transmission optimization study," [online]. Available: www.ercot.com.

[9] J.W. Ballance, S. Goldberg, "Subsynchronous Resonance in Series Compensated Transmission Lines," *IEEE Transactions on Power Apparatus and Systems,* vol. PAS-92, no. 5, pp. 1649-1658, Sept. 1973.

[10] P. M. Anderson, B. L. Agrawal and J. E. V. Ness, "Subsynchronous Resonance in Power Systems." New York, United States of America: IEEE Press, 1989.

[11] K. R. Padiyar, "Analysis of Subsynchronous Resonance in Power Systems." United States of America: Kluwer Academic Publisher, 1999.

[12] R.K. Varma, S. Auddy, Y. Semsedini, "Mitigation of Subsynchronous Resonance in a Series-Compensated Wind Farm Using FACTS Controllers," *IEEE Transactions on Power Delivery,* vol. 23, no. 3, pp. 1645-1654, Jul. 2008.

[13] M.S. El-Moursi, B. Bak-Jensen, M.H. Abdel-Rahman, "Novel STATCOM Controller for Mitigating SSR and Damping Power System Oscillations in a Series Compensated Wind Park," *IEEE Transactions on Power Electronics,* vol. 25, no. 2, pp. 429-441, Feb. 2010

[14] Z. Lubosny, *Wind Turbine Operation in Electric Power System.* New York: Springer, 2003.

[15] P. M. Anderson and R. Farmer, "Series Compensation of Power Systems." United States of America: PBLSH! Inc., 1996,

[16] IEEE SSR Working Group, "Terms, Definitions and Symbols for Subsynchronous oscillations," *IEEE Trans.*, vol. PAS-104, June 1985.
[17] M. C. Hall and D. A. Hodges, "Experience with 500-kV Subsynchronous Resonance and Resulting Turbine Generator Shaft Damage at Mohave Generating Station," *IEEE PES Special Publication, Analysis and Control of Subsynchronous Resonance, IEEE Publication 76 CH 1066-0-PWR*, pp. 22–29, 1976.
[18] G. Anderson, R. Atmuri, R. Rosenqvist and S. Torseng, "Influence of Hydro Units Generator-to-Turbine Ratio on Damping of Subsynchronous Oscillations," IEEE Trans., v. PAS-103, n.4, Aug. 1984, pp. 2352-2361.
[19] L. Harnefors, M. Bongiorno and S. Lundberg, "Input-Admittance Calculation and Shaping for Controlled Voltage-Source Converters, " IEEE Transactions on Industrial Electronics, vol. 54, no. 6, pp. 3323-3334, Dec. 2007.
[20] L. Harnefors and M. Bongiorno, "Current Controller Design for Passivity of the Input Admittance," in Proc. of 13th European Conference on Power Electronics and Applications, 2009 (EPE '09), September 8-10, 2009, Barcelona, Spain.
[21] R. G. Farmer, A. L. Schwalb, and E. Katz, "Navajo project report on subsynchronous resonance: analysis and solution," IEEE Trans., vol. PAS-96, no. 1, pp. 1226–1232, 1977.
[22] N. G. Hingorani, B. Bhargava, G. F. Garrigue, and G. D. Rodrigues, "Prototype NGH subsynchronous resonance damping scheme. Part I - field installation and operating experience," IEEE Trans. on Power Syst., vol. PWRS-2, no. 4, pp. 1034–1039, 1987.
[23] N. G. Hingorani and L. Gyugyi, Understanding FACTS. Concepts and technology of Flexible AC Transmission Systems. New York: IEEE Press, 2000.
[24] K. R. Padiyar and N. Prabhu, "Analysis of subsynchronous resonance with three level twelve-pulse VSC based SSSC," in Proc. Of Conference on Convergent Technologies for Asia-Pacific Region (TENCON), 2003, vol. 1, Oct. 2003, pp. 76–80.
[25] K. Ahlgren, D. Holmberg, P. Halvarsson, and L. Ängquist, "Thyristor controlled series capacitor used as a means to reduce torsional interaction subsynchronous resonance," in Proc. of Cigré SC14 Colloquium on HVDC and FACTS in South Africa, 1997.
[26] G. N. Pillai, A. Ghosh, and A. Joshi, "Robust control of SSSC to improve torsional damping," in Proc. of 38th IEEE Power Engineering Society Winter Meeting, 2001, vol. 3, Jan. 2001, pp. 1115–1120.
[27] M. Bongiorno, J. Svensson and L. Ängquist, "Single-phase VSC Based SSSC for Subsynchronous Resonance Damping," IEEE Transactions on Power Delivery, vol. 23, no. 3, pp. 1544-1552, July 2008.
[28] T. Burton, D. Sharpe, N. Jenkins and E. Bossanyi, Wind Energy Handbook, Chichester: John Wiley & Sons, 2001.
[29] A. Petersson, "Analysis, Modeling and Control of Doubly-Fed Induction Generators for Wind Turbines," Ph.D. dissertation, Dept. of Energy and Environ., Chalmers Univ. of Technol., Göteborg, Sweden 2005.
[30] A. Tabesh and R. Iravani, "Small-Signal Dynamic Model and Analysis of a Fixed-Speed Wind Farm - A Frequency Response Approach,"

IEEE Trans. On Power Delivery, vol. 21, no. 2, April 2006, pp. 778-787.
[31] T. Ackermann and L. Söder, "An overview of wind energy-status 2002," Renew. Sustain. Energy Rev., vol. 6, no. 1–2, pp. 67–128, Feb./Apr. 2002.
[32] "8Belkin_Event," [online]. Available: http://www.ercot.com/content/meetings/rpg-crez/keydocs/2010/0126/8Belkin_Event%20of%2010.ppt.
[33] Siemens PTI, "PSSETM 30.2 USERS MANUAL," November 2005.
[34] K. Thorborg, "Power Electronics – in Theory and Practice," Lund: Studentlitteratur, 1997.
[35] N. Mohan, T. Undeland and W. Robbins, "Power Electronics," Canada: John Wily and Sons, Inc., 1995.
[36] M. Bongiorno, J. Svensson and L. Ängquist, "Online Estimation of Subsynchronous Voltage Components in Power Systems," IEEE Trans. on Power Delivery, vol. 23, no. 1, pp. 410-418, Jan. 2008.
[37] O. Wallmark and L. Harnefors, "Sensorless control of salient PMSM drives in the transition region," IEEE Trans. on Industrial Electron., vol. 53, no. 4, pp. 1179–1187, Aug. 2006.

8 Nomenclature

8.1 Abbreviations

SSR	Subsynchronous Resonance
IGE	Induction Generator Effect
TI	Torsional Interaction
TA	Torque Amplification
FACTS	Flexible AC Transmission Systems
DFIG	Doubly-Fed Induction Generator
IG	Induction Generator
VSC	Voltage Source Converter
WT	Wind Turbine
PLL	Phase-Locked Loop

ELFORSK

SVENSKA ELFÖRETAGENS FORSKNINGS- OCH UTVECKLINGS - ELFORSK - AB

Elforsk AB, 101 53 Stockholm. Besöksadress: Olof Palmes Gata 31
Telefon: 08-677 25 30, Telefax: 08-677 25 35
www.elforsk.se